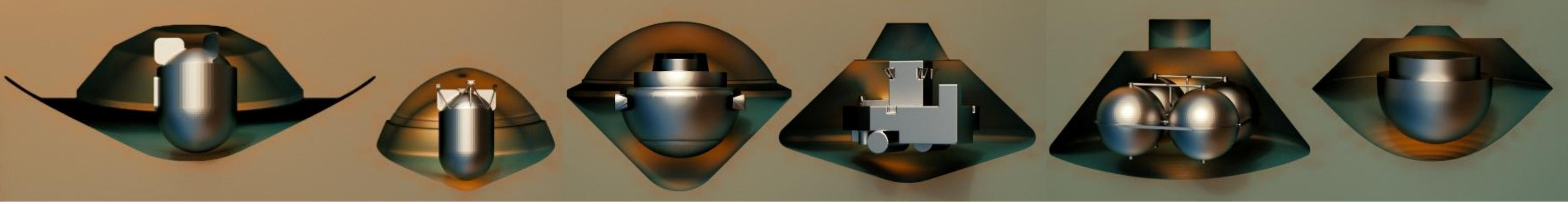

Entry, Descent, and Landing Systems Short Course

Subject: Aerodynamics & Aerothermodynamics

Authors: Karl Edquist & Mark Schoenenberger
NASA Langley Research Center
Mike Wright
NASA Ames Research Center

sponsored by
International Planetary Probe Workshop 10
June 15-16, 2013
San Jose, California

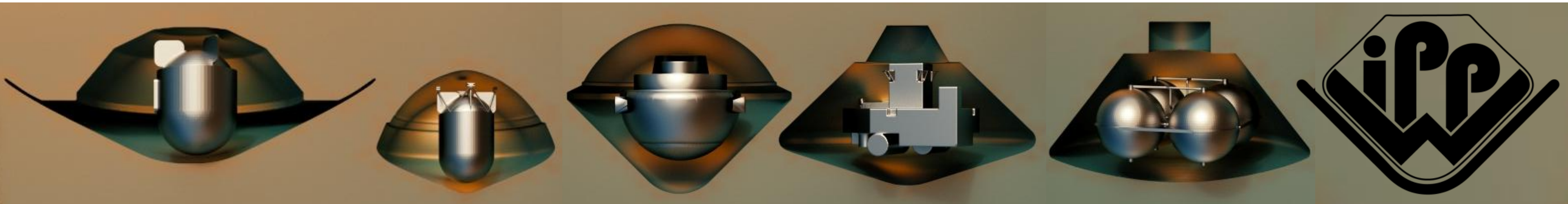

Outline

- Aerodynamics
  - Introduction/History/Methods
  - Dynamic Stability
- Aerothermodynamics
  - Introduction
  - Methods
  - Special Topics
- Case Study: MSL
- Q&A

- Material focuses on blunt rigid capsules

Aerodynamics

Definitions

Aerodynamics = forces & moments imparted on the entry vehicle by the atmosphere

Primary EDL Needs: High C_D, Static stability ($dC_m/d\alpha < 0$)

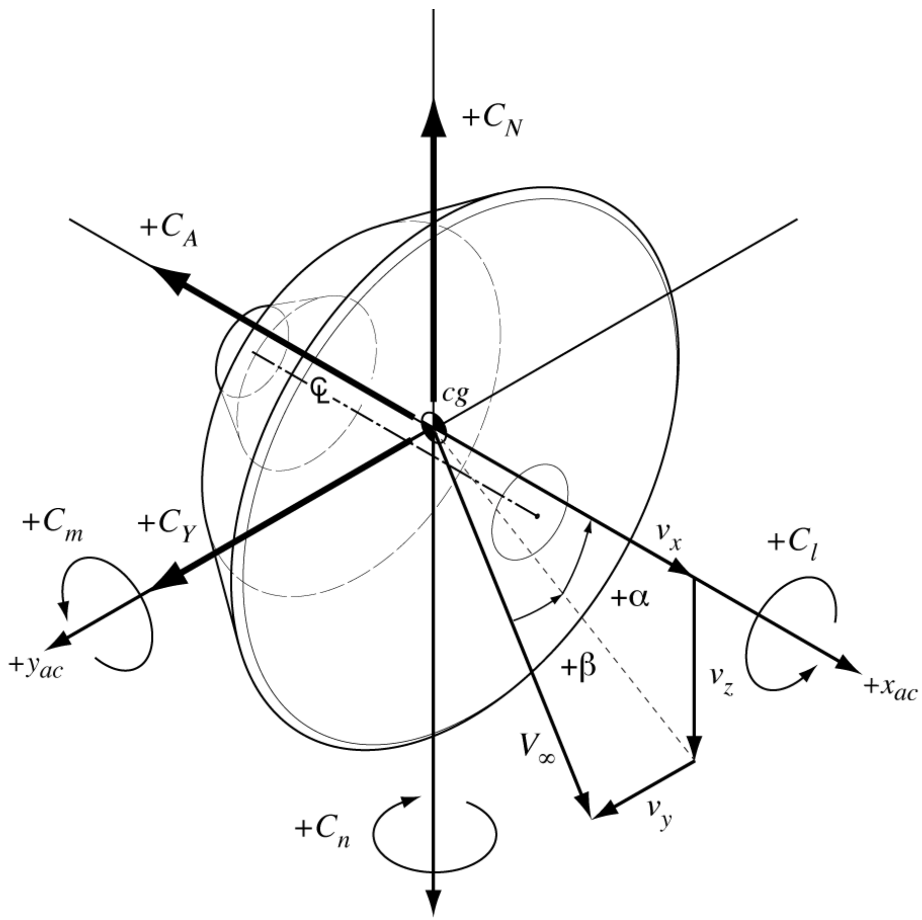

Force Coefficient

$$C_X = \frac{F_X}{\frac{1}{2}\rho_\infty V_\infty^2 S_{ref}}$$

Moment Coefficient

$$C_x = \frac{M_x}{\frac{1}{2}\rho_\infty V_\infty^2 S_{ref} d_{ref}}$$

$$F = \int_{surface} (pressure + shear)$$

$$M = \int_{surface} (pressure + shear) \times (l - l_{ref})$$

Lift Coefficient $C_L = C_N \cos\alpha - C_A \sin\alpha$

Drag Coefficient $C_D = C_N \sin\alpha + C_A \cos\alpha$

Pitch and Yaw Damping Coefficients

$$C_{m_q} + C_{m_{\dot\alpha}} = \frac{\partial C_m}{\partial \frac{q d_{ref}}{2V_\infty}} + \frac{\partial C_m}{\partial \frac{\dot\alpha d_{ref}}{2V_\infty}}$$

$$C_{n_r} - C_{n_{\dot\beta}} = \frac{\partial C_n}{\partial \frac{r d_{ref}}{2V_\infty}} - \frac{\partial C_n}{\partial \frac{\dot\beta d_{ref}}{2V_\infty}}$$

The Blunt-Body Arsenal* [2-37]

- **EDL vehicles generally have blunt heatshields → high aerodynamic drag**
- **Other geometry drivers: packaging, stability, heating, science**
- **Backshells are generally selected to accommodate payload**

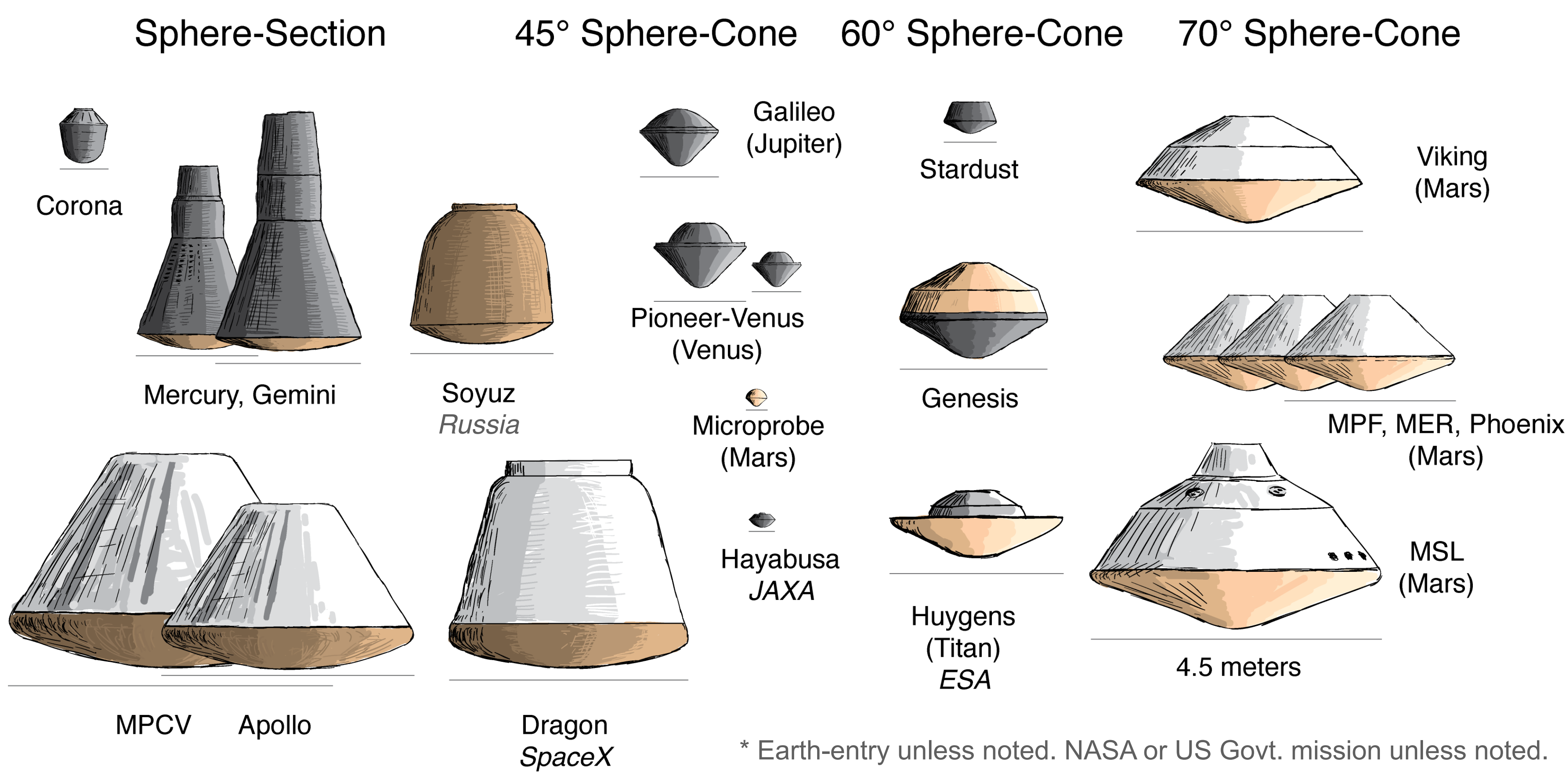

* Earth-entry unless noted. NASA or US Govt. mission unless noted.

Flight Regimes (e.g. MSL)

Each flight regime requires unique prediction methods

ENTRY (V=5.8 km/s) — Parachute Deploy (V=0.5 km/s)

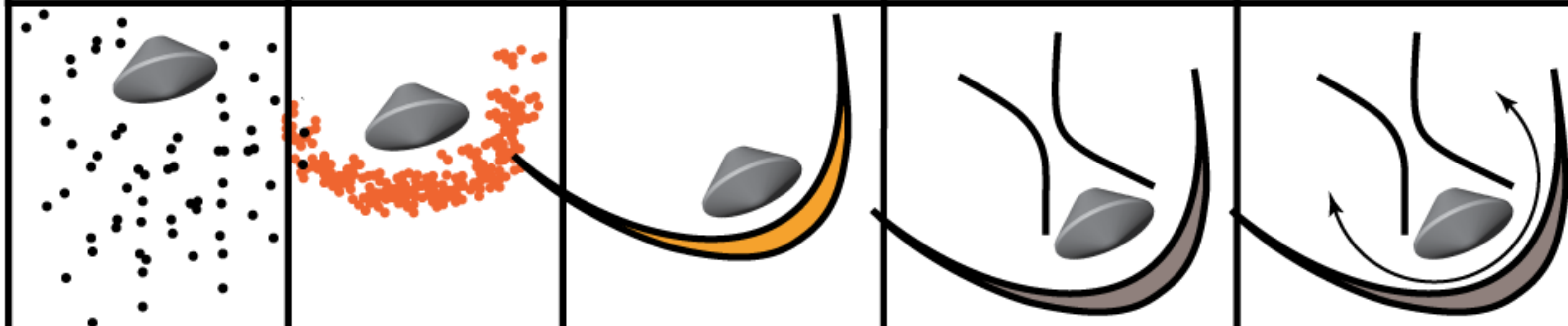

	Rarefied	Transitional	Hypersonic	Supersonic	Supersonic Dynamics
Regime Definition	Knudsen > 1000	1000 > Kn > 0.001	26.6 > Mach > 6	6 > Mach > 1.5	3.5 > Mach > 1.5
Data Source:	DAC DSMC code	DAC DSMC code	LAURA CFD (forebody)	LAURA (full aeroshell) w/ base correction	Ballistic Range Data
Characteristic Flow Physics	Molecules do not collide	Molecular collisions modeled, still not continuum flow	Chemically reacting flow Peak heating, Peak dynamic pressure	Wake aerodynamics contribute to capsule forces/moments	Unsteady wake introduces capsule dynamic instabilities
New Technical Challenges for MSL	Uncertainties for Lifting Vehicle	Uncertainties for Lifting Vehicle	Uncertainties for Lifting Vehicle	Uncertainties for Lifting Vehicle	Uncertainties for Lifting Vehicle
			RCS interactions	RCS interactions	
			Higher L/D aerodynamics	Higher L/D aerodynamics	Higher L/D aerodynamics
			Aero-load deformation Ablation shape change	Balance Mass Jettison	Lifting pitch/yaw damping

Newtonian Aerodynamics [38,39]

Newtonian method is an approximate method for estimating static aerodynamic coefficients
Newtonian method is more accurate for blunt bodies at hypersonic conditions

$$\dot{m} = \rho_\infty V_\infty A \sin\theta$$

$$V_N = V_\infty \sin\theta$$

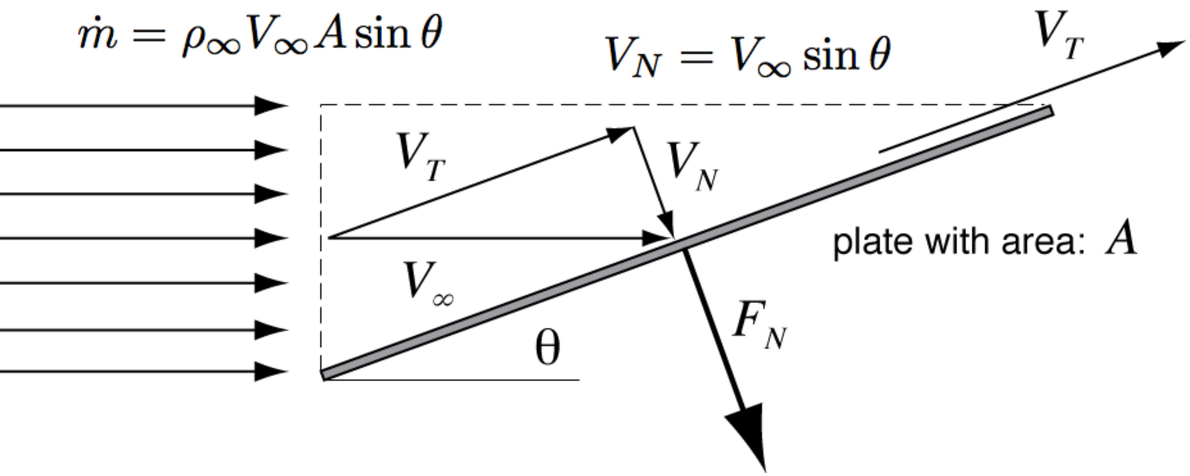

$$F = \dot{m} V_N = \rho_\infty A V_\infty^2 \sin^2\theta$$

$$\frac{F}{A} = \rho_\infty V_\infty^2 \sin^2\theta = p - p_\infty$$

$$\boxed{C_p = \frac{p - p_\infty}{\frac{1}{2}\rho_\infty V_\infty^2} = \frac{2V_N^2}{V_\infty^2} = 2\sin^2\theta}$$

Lester Lees [40]: Updated Newtonian model replacing “2” with the maximum Cp based on Rayleigh Pitot equation (normal-shock relations), experiment or CFD.

Modified Newtonian “sine-squared law:”

$$\boxed{C_p = C_{p_{max}} \sin^2\theta}$$

$$C_{p_{max}} = 1.839 \text{ for } \gamma = 1.4$$

Modified Newtonian Aerodynamics

From Lees [40]

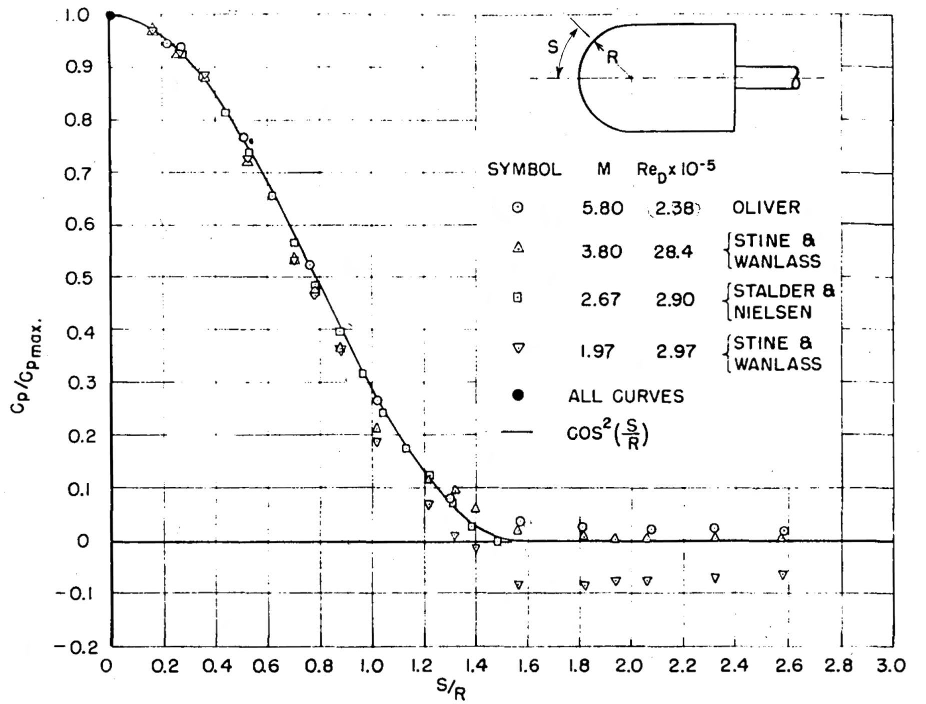

FIG. 13 - PRESSURE COEFFICIENT DISTRIBUTION ON SURFACE OF HEMISPHERE-CYLINDER AT VARIOUS MACH NUMBERS

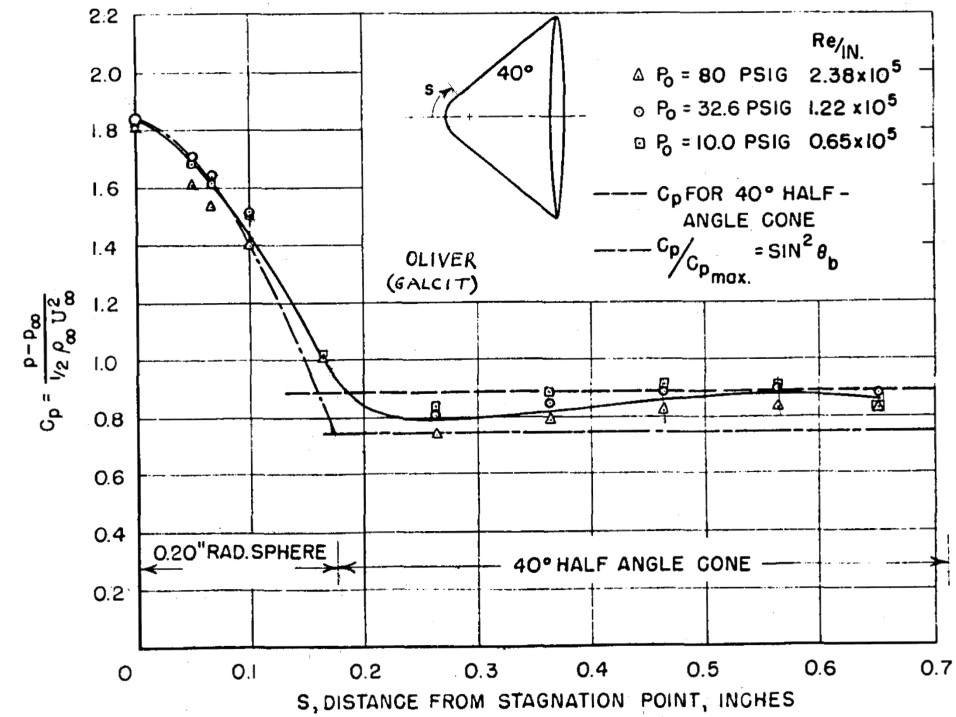

FIG. 14 - PRESSURE DISTRIBUTION OVER BLUNT CONE, $M_\infty = 5.8$, $\alpha = 0°$

For hypersonic flows, local pressure is a function of the local surface angle relative to the flow

Blunt Body Aerodynamic Characteristics

Modified Newtonian, Air, Mach = 20

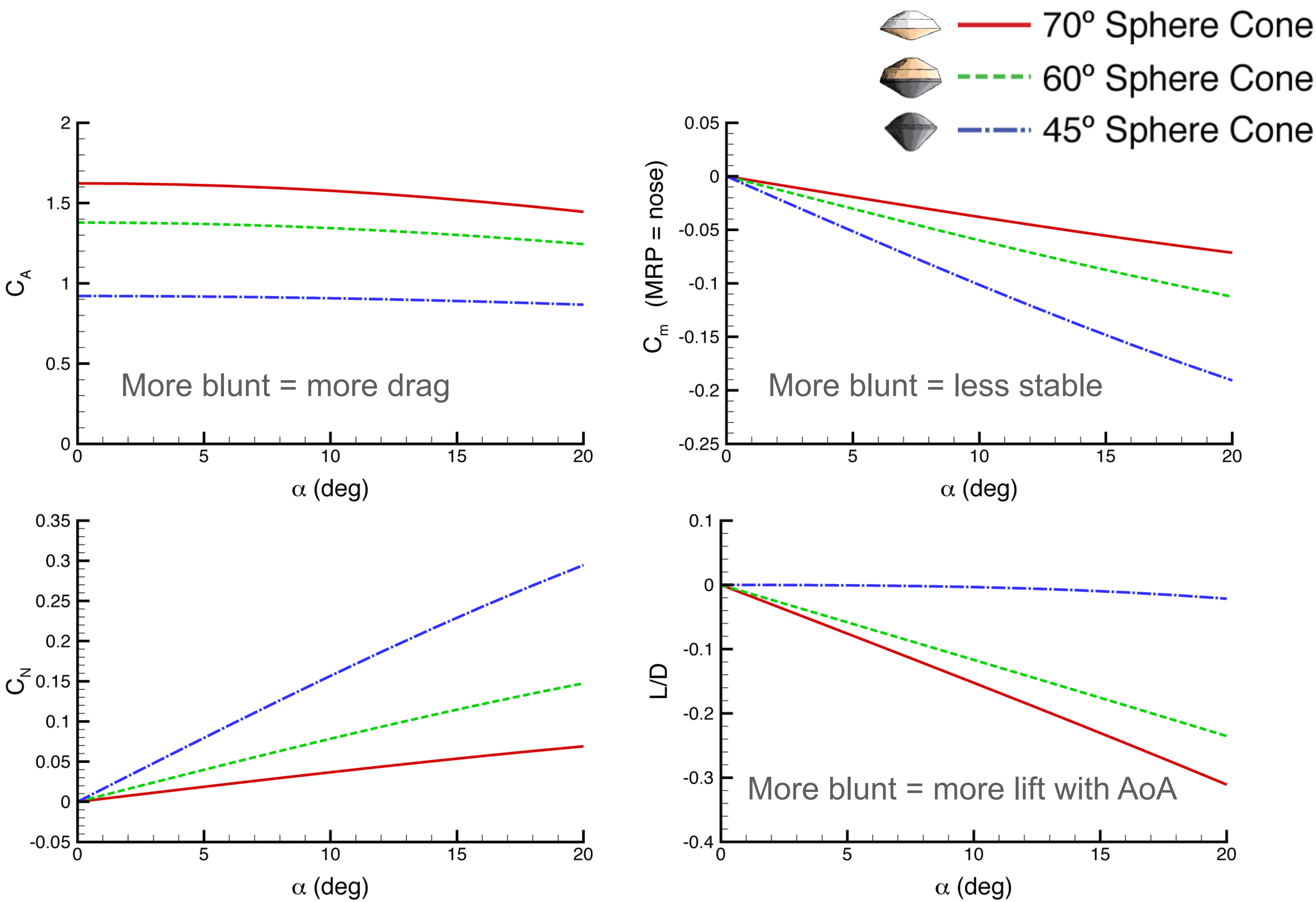

Viking Design vs. Flight Trim AOA and L/D [17]

- Viking was designed for L/D = 0.18 at a hypersonic trim AOA of 11 deg
- Aerodynamics were predicted from wind tunnel and ballistic range tests in air, CO2, CF4
- VL1 and VL2 trim AOA (and L/D) were higher than the design values
  - Believed at the time to be caused by an off-nominal CG location and outgassing/ ablation at the time, although low heat flux was experienced

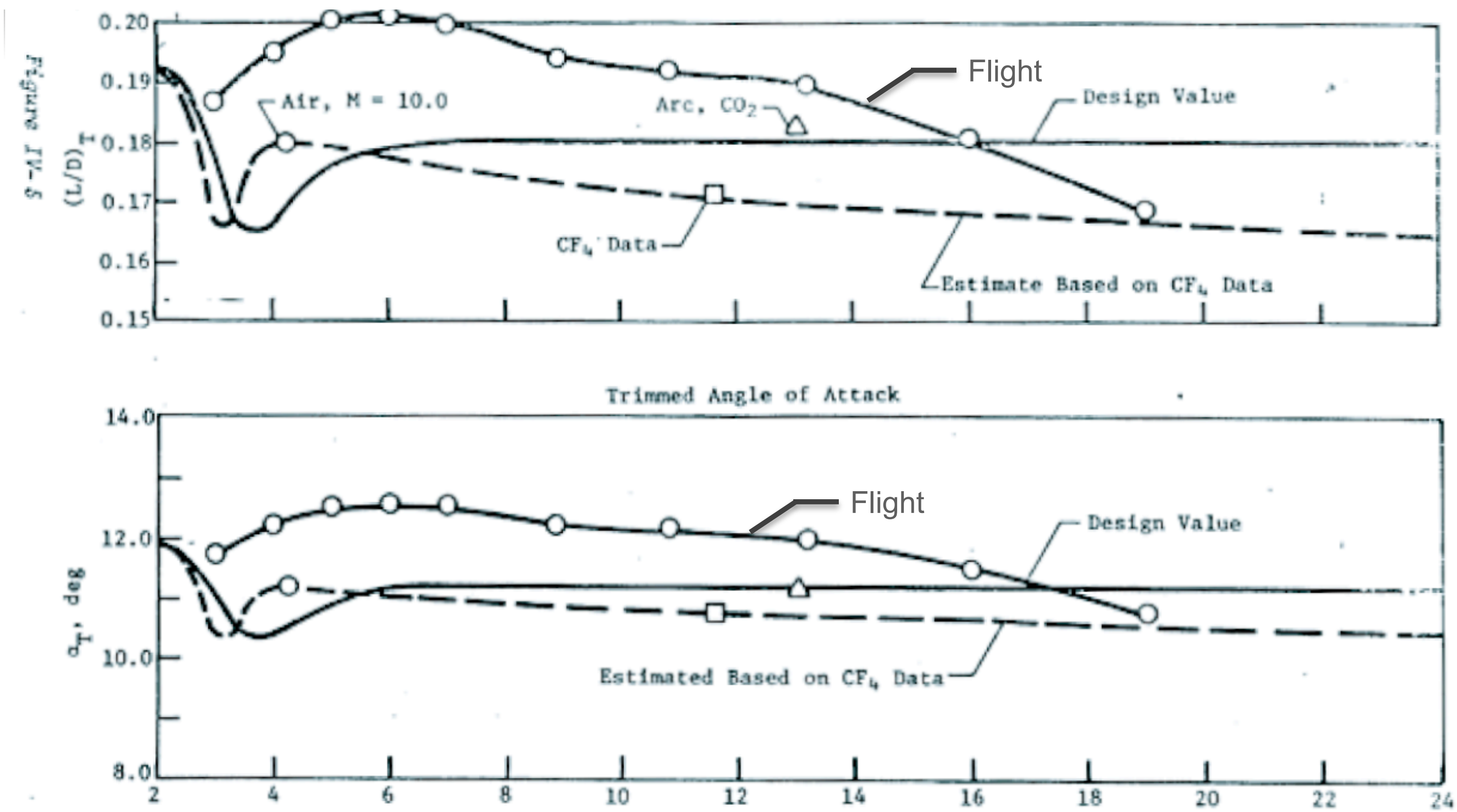

National Aerodynamic Experimental Facilities

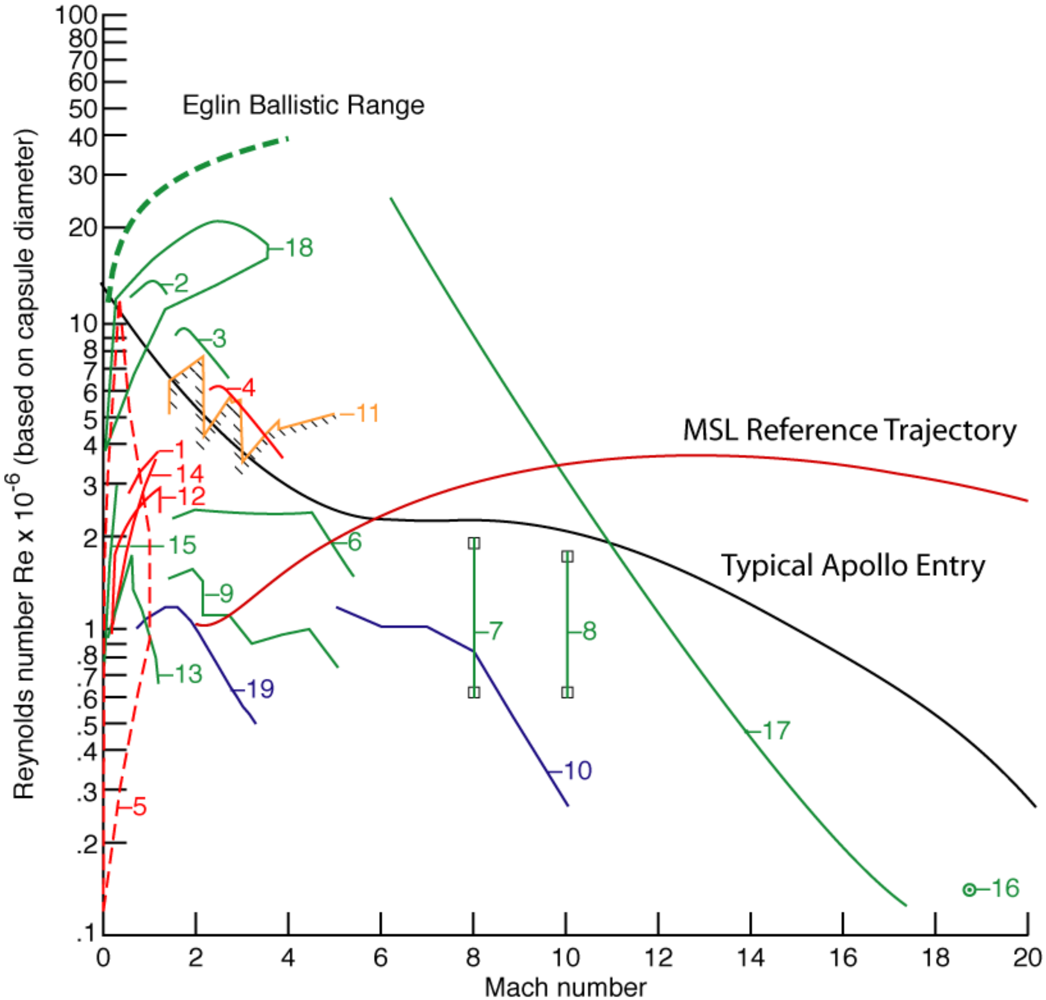

1. Ames 14-Ft Transonic wind Tunnel (0.055 scale)
   Ames Unitary Plan Wind Tunnels (0.105 scale)
2. 11 by 11 ft
3. 9 by 7 ft
4. 8 by 7 ft
5. Ames 12-Ft Pressure Tunnel (0.10 scale)
6. Arnold Engineering Development Center, von Karman Facility 50-In. Tunnel A (0.045 scale)
7. Arnold Engineering Development Center, von Karman Facility 50-In. Tunnel B (0.045 scale)
8. Arnold Engineering Development Center, von Karman Facility 50-In. Tunnel C (0.045 scale)
9. Jet Propulsion Laboratory 20-In. Supersonic Wind Tunnel (0.045 scale)
10. Jet Propulsion Laboratory 21-In. Hypersonic Wind Tunnel (0.02 scale)
11. Langley Unitary Plan Wind Tunnel (0.055 scale)
12. Langley 8-Ft Transonic Pressure Tunnel (0.055 scale)
13. Langley 16-Ft Transonic Dynamics Tunnel (0.08 scale)
14. Langley 16-Ft Transonic Wind Tunnel (0.085 scale)
15. North American Aerodynamics Laboratory 7- by 10-ft Low-Speed Wind Tunnel (0.105 scale)
16. Arnold Engineering Development Center, von Karman Facility 50-In. Hot-Shot II, Tunnel H (0.04 scale)
17. Cornell Aeronautical Laboratory 48-in. Shock Tunnel (0.05 scale)
18. North American Aviation 7- by 7-ft Trisonic Wind Tunnel (0.105 scale)
19. North American Aviation Supersonic Aerophysics Laboratory (0.02 scale)

From [10] NASA TN-D 3748, "Apollo Wind Tunnel Testing Program Historical Development of General Configurations"

National Aerodynamic Experimental Facilities

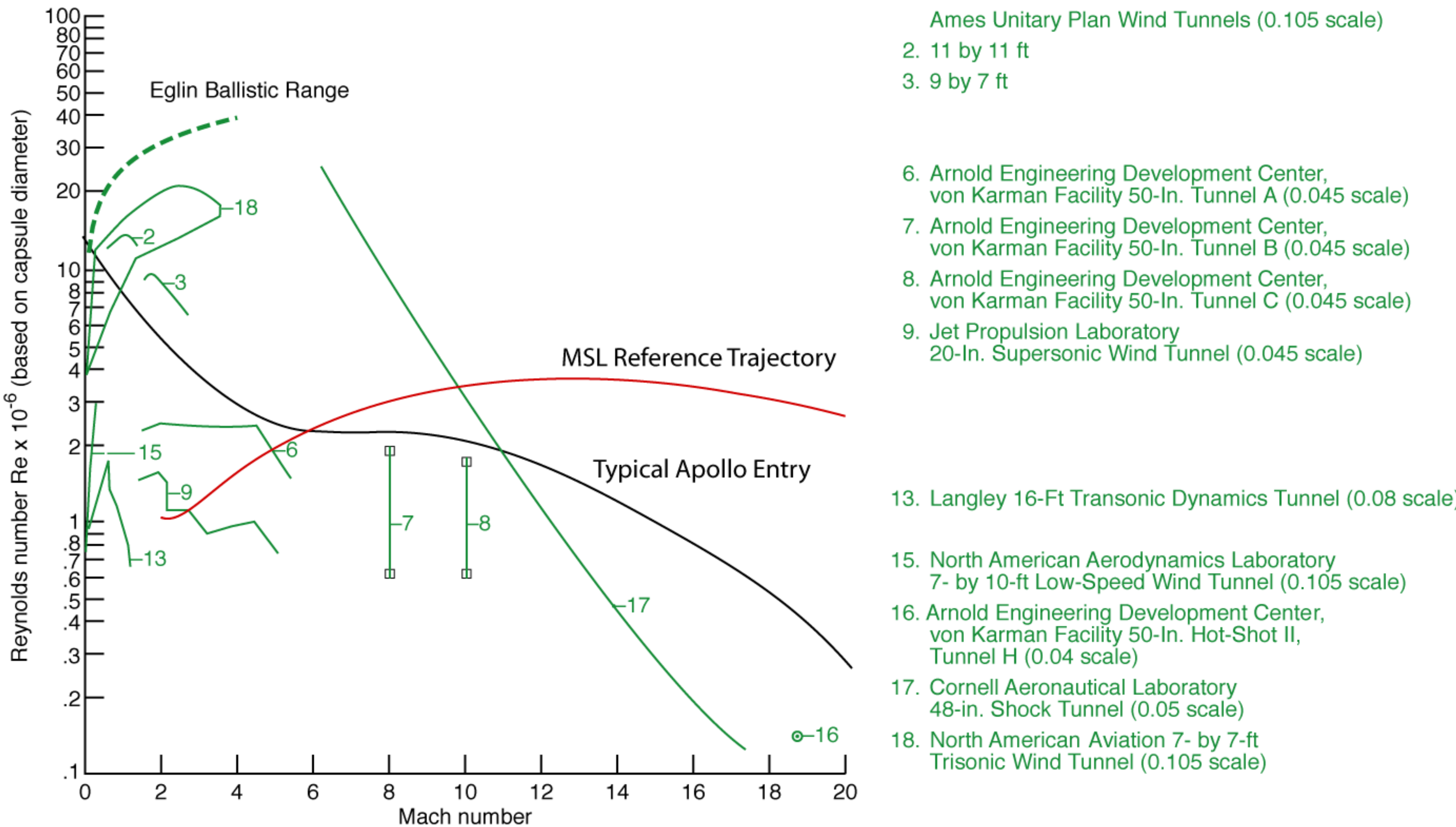

From [10] NASA TN-D 3748, "Apollo Wind Tunnel Testing Program Historical Development of General Configurations"

Computational Fluid Dynamics (CFD)

- Definition: Numerical solution of the fluid dynamic equations of motion
- The closing of wind tunnels & advancement of computers has pushed CFD to the forefront of aerothermodynamics prediction
  - CFD is a high-fidelity method of "simulating" flight conditions (esp. hypersonic)
- But, the resources required can be large (people, time, computers), especially for complex 3-D geometries
- Examples: LAURA (NASA Langley), DPLR (NASA Ames)

Vehicle Geometry

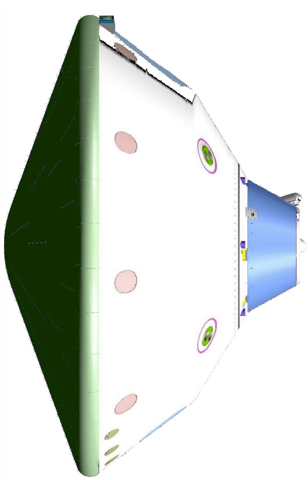

CFD Grid

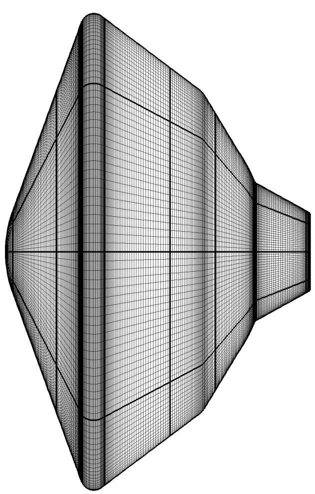

Navier-Stokes Equations

Continuity equation

$$\frac{\partial \rho}{\partial t} + \nabla \cdot (\rho \mathbf{V}) = 0$$

x Momentum

$$\rho \frac{Du}{Dt} = -\frac{\partial p}{\partial x} + \frac{\partial \tau_{xx}}{\partial x} + \frac{\partial \tau_{yx}}{\partial y} + \frac{\partial \tau_{zx}}{\partial z}$$

y Momentum

$$\rho \frac{Dv}{Dt} = -\frac{\partial p}{\partial y} + \frac{\partial \tau_{xy}}{\partial x} + \frac{\partial \tau_{yy}}{\partial y} + \frac{\partial \tau_{zy}}{\partial z}$$

z Momentum

$$\rho \frac{Dw}{Dt} = -\frac{\partial p}{\partial z} + \frac{\partial \tau_{xz}}{\partial x} + \frac{\partial \tau_{yz}}{\partial y} + \frac{\partial \tau_{zz}}{\partial z}$$

Energy

$$\rho \frac{D(e + V^2/2)}{Dt} = \rho \dot{q} + \frac{\partial}{\partial x}\left(k \frac{\partial T}{\partial x}\right) + \frac{\partial}{\partial y}\left(k \frac{\partial T}{\partial y}\right) + \frac{\partial}{\partial z}\left(k \frac{\partial T}{\partial z}\right) - \nabla \cdot p\mathbf{V}$$
$$+ \frac{\partial (u\tau_{xx})}{\partial x} + \frac{\partial (u\tau_{yx})}{\partial y} + \frac{\partial (u\tau_{zx})}{\partial z} + \frac{\partial (v\tau_{xy})}{\partial x} + \frac{\partial (v\tau_{yy})}{\partial y}$$
$$+ \frac{\partial (v\tau_{zy})}{\partial z} + \frac{\partial (w\tau_{xz})}{\partial x} + \frac{\partial (w\tau_{yz})}{\partial y} + \frac{\partial (w\tau_{zz})}{\partial z}$$

CFD Output

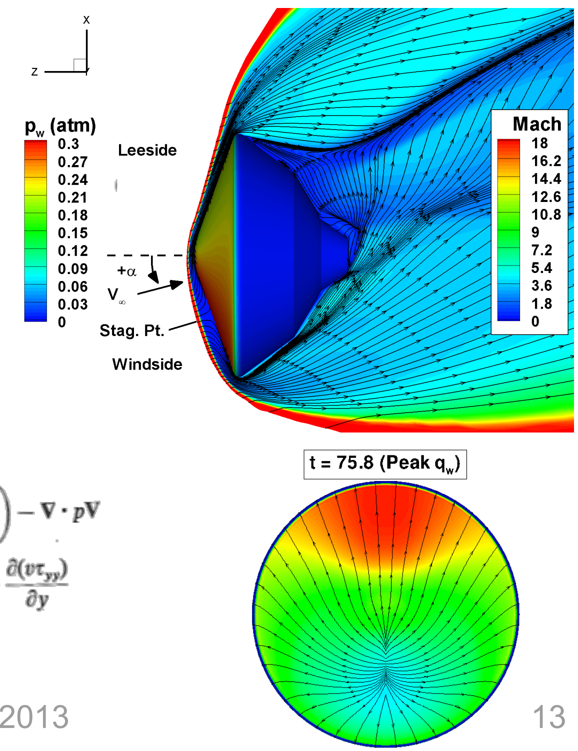

Dynamic Stability

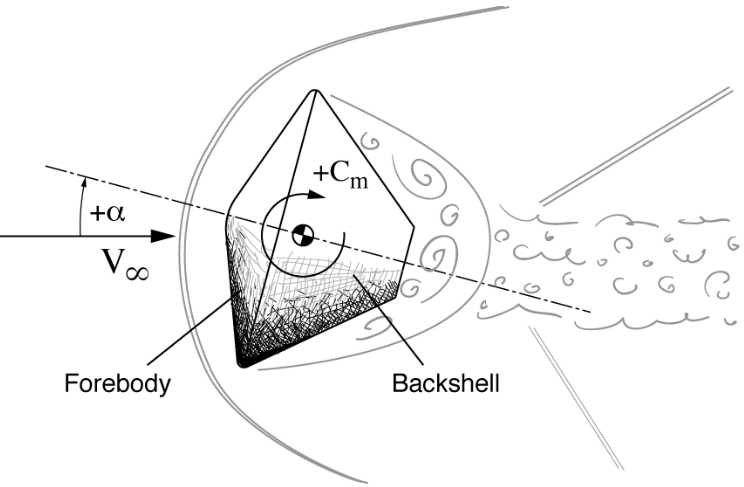

- Blunt bodies are dynamically unstable at supersonic speeds - driven by wake flow
- Phenomenon starts around Mach 3.5 and slower
- Stability can vary dramatically with backshell shape
- Unsteady CFD has provided insight on flow mechanisms
- Experiment is the only validated method of determining pitch damping coefficients

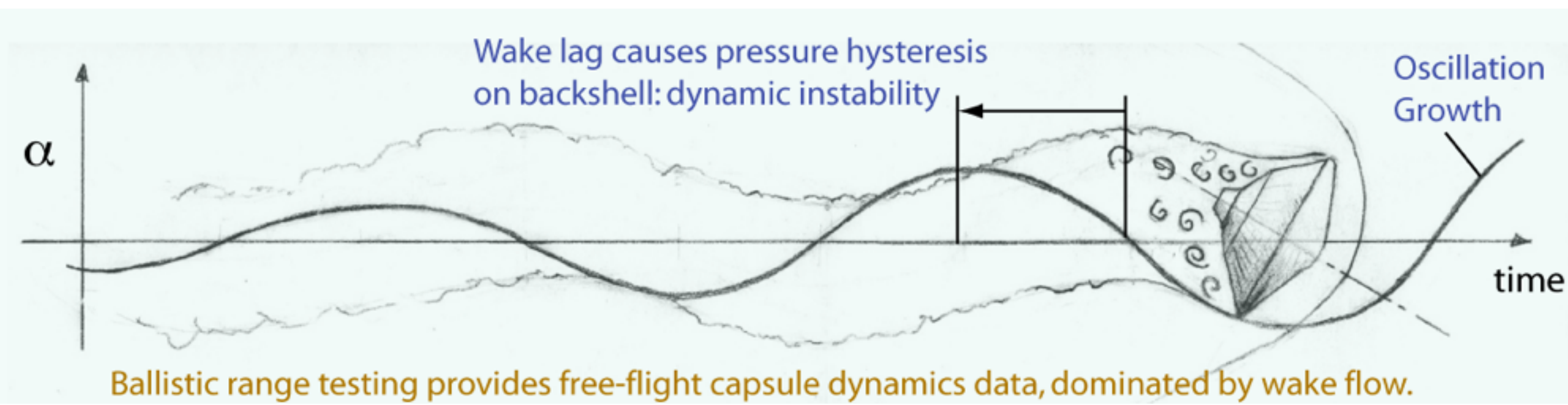

Free Flight Dynamic Stability Test Facilities

NASA Ames HFFAF (can test lifting, but Re is typically low)

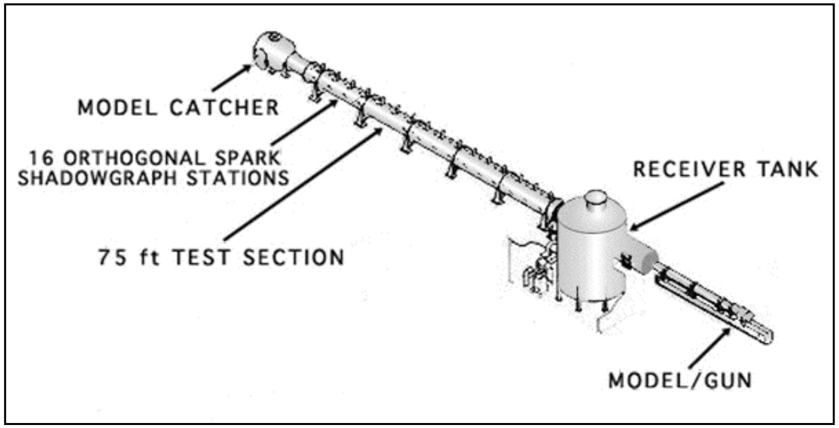

Eglin Air Force Base: Aeroballistic Test and Evaluation Facility (ATEF)
(Used for all recent robotic missions but currently mothballed)

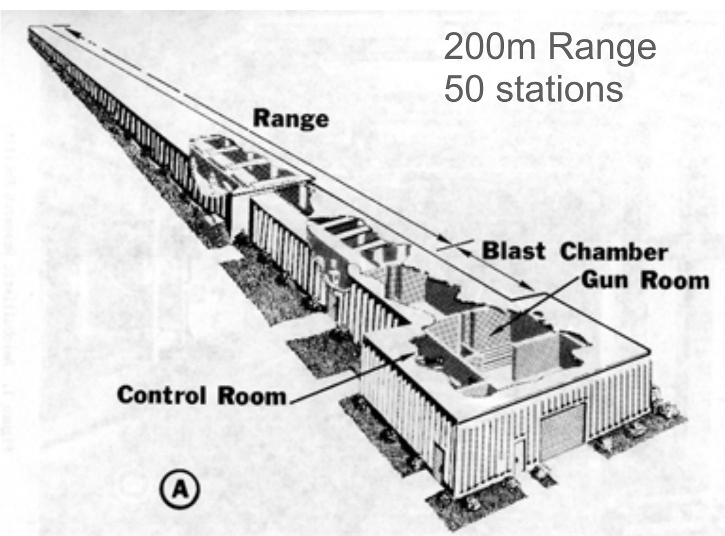

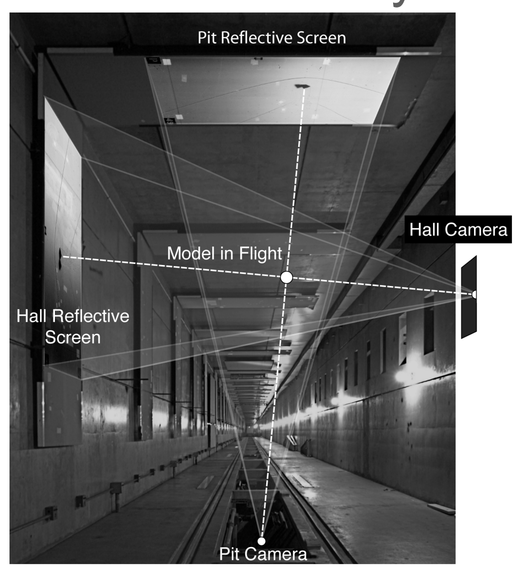

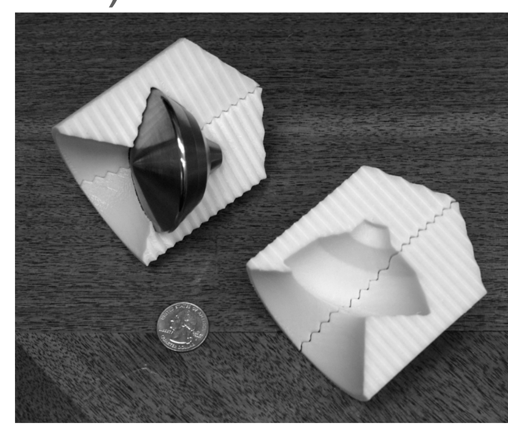

MSL model

Mars Pathfinder Reconstruction

Statics: LAURA CFD
Dynamics: Ballistic Range

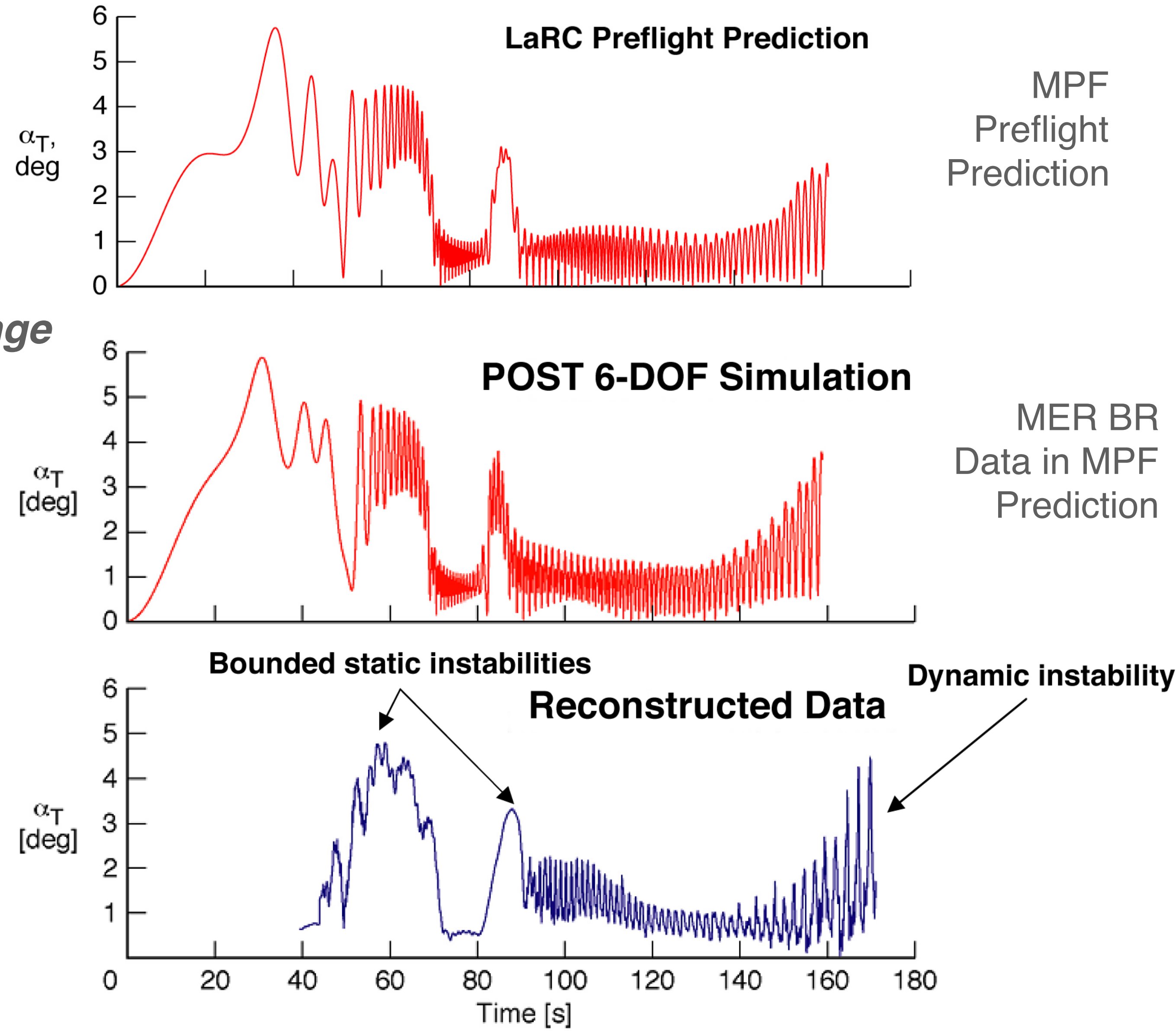

MPF Preflight Prediction

MER BR Data in MPF Prediction

MPF Flight Data Reconstruction

[24] AIAA-2005-0055

Aerothermodynamics

What is Aerothermodynamics?

- Definition: Aerodynamic heating of a solid surface by a gas through a viscous boundary layer & high-temperature shock layer
  - First addressed in the 1950s with the advent of hypersonic re-entry missiles
- Aerodynamic heating is most often associated with hypersonic atmospheric flight → high velocity + dense atmospheric gas = high temperatures

Apollo

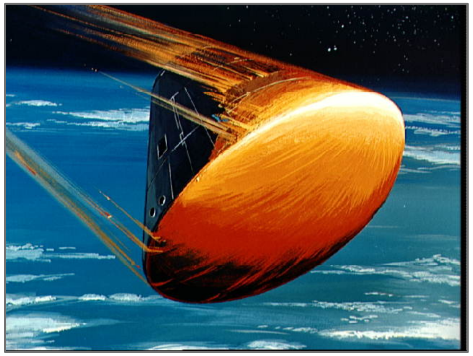

Space Shuttle

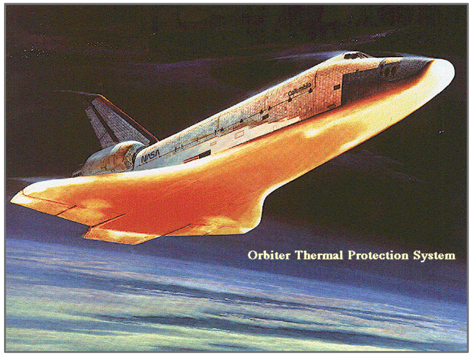

Pioneer Venus

Mars Science Laboratory

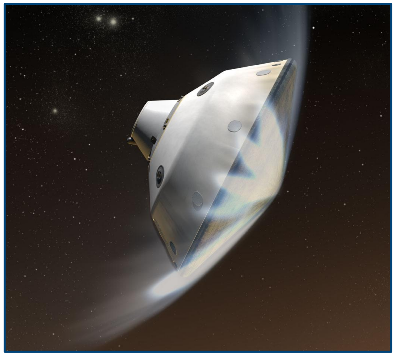

"Two major problems encountered today in aeronautics are the determination of skin friction and skin temperatures of high-speed aircraft."
E. R. Van Driest, 1950

Thermal Protection

- Entry vehicle kinetic energy → increased shock layer temperature → increased surface temperature
- Payloads, human or robotic, must be protected from extreme temperatures
- Load-bearing structures cannot perform adequately at elevated temperatures
  - Material performance degrades
- The type & amount of <u>thermal protection system</u> (TPS) material depend on the prediction of aerodynamic heating at flight conditions
  - Heating = f(time), surface pressure & shear stress may also be important
  - Difficult/impossible to simulate flight conditions in ground facilities
- TPS adds mass to the EDL system!

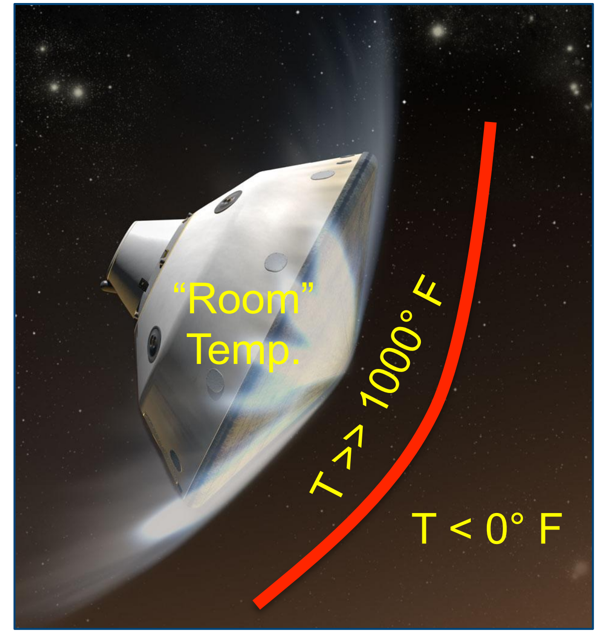

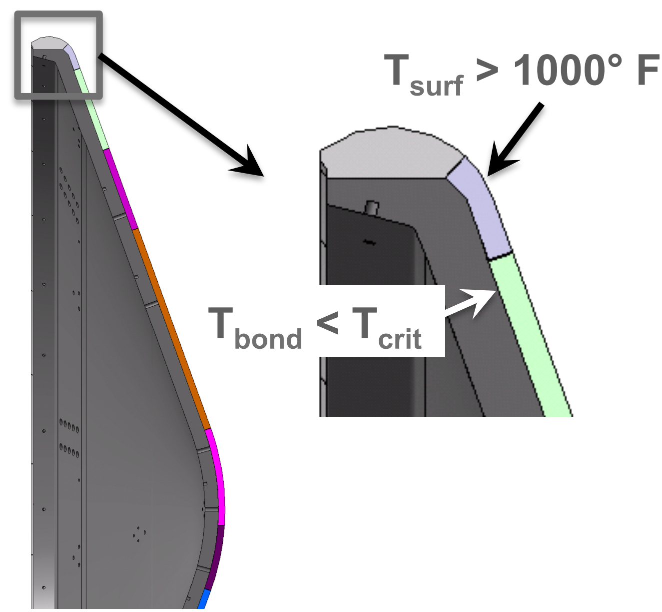

Terminology

- <u>Convection</u> = heat transfer via <u>conduction</u> & <u>diffusion</u> through a <u>viscous boundary layer</u>
  - Conduction ~ Temperature gradient at surface
  - Diffusion (aka Catalytic Heating) ~ Gas/surface chemical reactions
- <u>Radiation</u> = heat transfer via <u>atomic excitation</u> in a high-temperature shock layer
  - Radiation ~ Shock layer temperature

$$q_w = \overbrace{q_{Cond} + q_{Diff}}^{\textbf{Convection}} + \overbrace{q_{Rad}}^{\textbf{Radiation}}$$

- <u>Heat rate</u> (q_w) = instantaneous heat transfer (W/cm^2)
- <u>Heat load</u> ($Q_w = \int q_w \, dt$) = integration of q_w (J/cm^2)
- Convective & radiative heating magnitudes depend on the entry vehicle & conditions
  - Mars: mostly convective
  - Earth (lunar return), Venus, Jupiter: convective & radiative

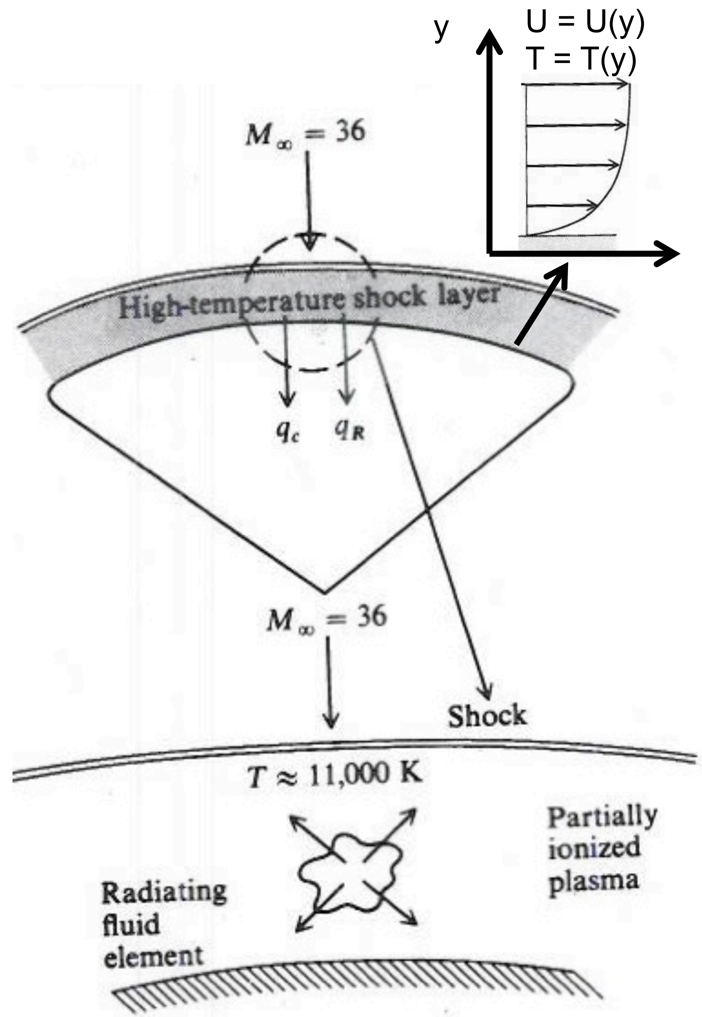

Schematic of Aerodynamic Heating to a Blunt Body (Ref. Anderson)

Engineering Methods

- Definition: Analytical solutions to the boundary layer equations
- Entry vehicles can be approximated by simple geometries
  - Nose (hemisphere), leading edge (cylinder), surface (cylinder or flat plate)
- Engineering methods have an important place in conceptual vehicle design
  - Quick to use, based on theory, can be integrated into trajectory codes
- Examples for stagnation point heating:
  - Requires effective nose radius (R_n)

Simplified Entry Vehicle Geometries

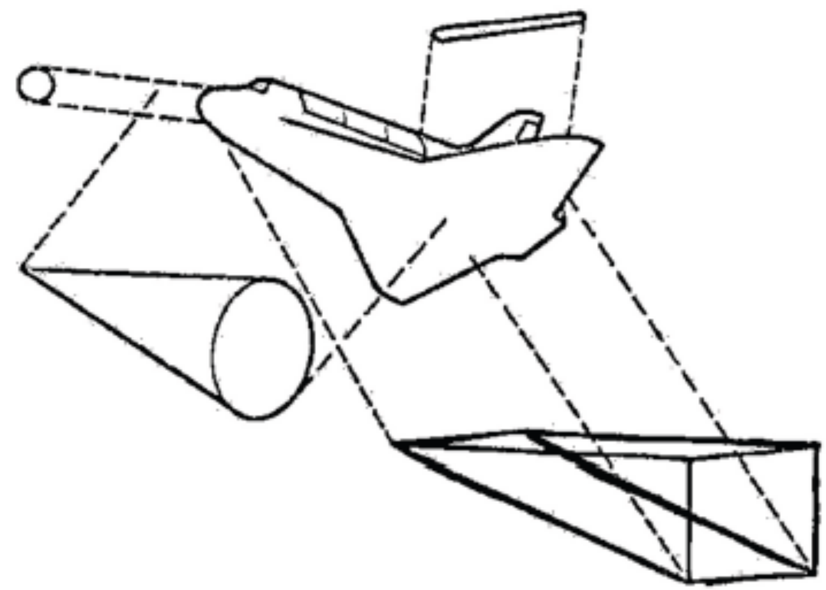

Fay & Riddell (1958) $$\dot{q}_w = \frac{0.763}{(\mathrm{Pr}_w)^{0.6}}(\rho_e\mu_e)^{0.4}(\rho_w\mu_w)^{0.1}\left[(h_o)_e - h_w\right]\left[1+(Le^{0.52}-1)\frac{h_d}{(h_o)_e}\right]\left[\boxed{\left(\frac{du_e}{dx}\right)_t}\right]^{0.5}$$

~ $1/R_n$

Sutton & Graves (Convective) $$q_c = C\left(\frac{\rho_\infty}{R_n}\right)^{\frac{1}{2}} V_\infty^3$$

Earth: C = 1.7415e-4
Mars: C = 1.9027e-4

Tauber & Sutton (Radiative) $$q_r = C_i R_n^a \rho_\infty^m f_i\left(V_\infty\right)$$

Earth: a = 1, m = 1.2
Mars: a = 0.526, m = 1.2

Example: Mars, Effect of Flight Path Angle

- Assumptions: Sutton-Graves stagnation point heating ($R_n = R_{eff}$), ballistic entry, exponential atmospheric density
- A steeper FPA increases max. heat flux, but decreases heat load (TPS thickness)
  - Potential for TPS mass savings by using a steeper entry

BC = m/C_DA = 90 kg/m^2; V_e = 5.5 km/s

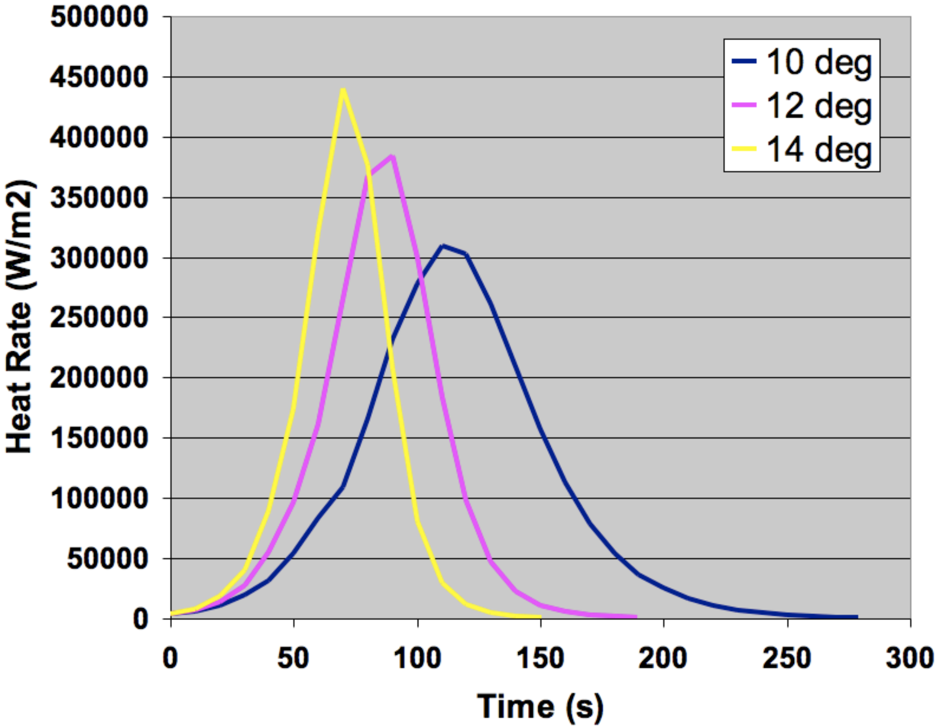

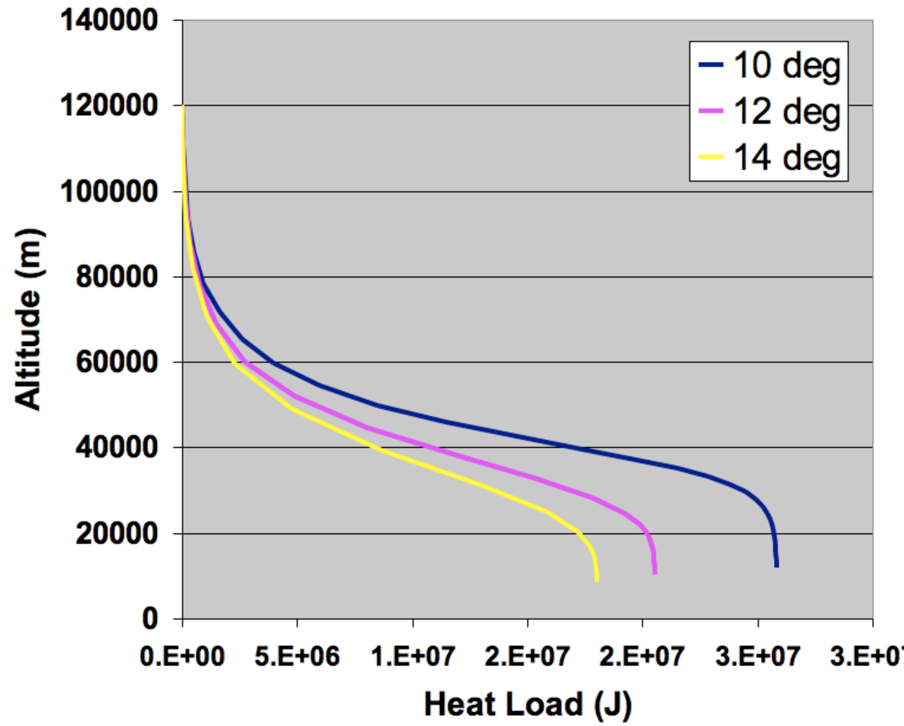

Example: Mars, Effect of Ballistic Coefficient

- Assumptions: Sutton-Graves stagnation point heating ($R_n = R_{eff}$), ballistic entry, exponential atmospheric density
- If the BC increases, heating will increase
  - Example: payload mass grows, but aeroshell diameter does not

$BC = m/C_DA$, γ_e = -12 deg, V_e = 5.5 km/s

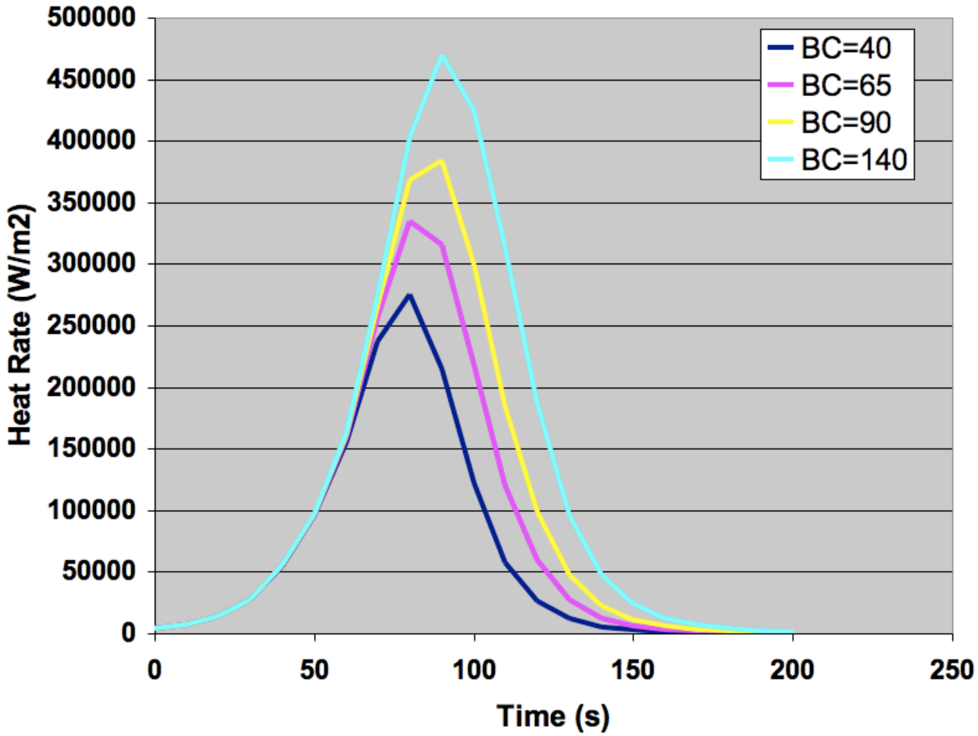

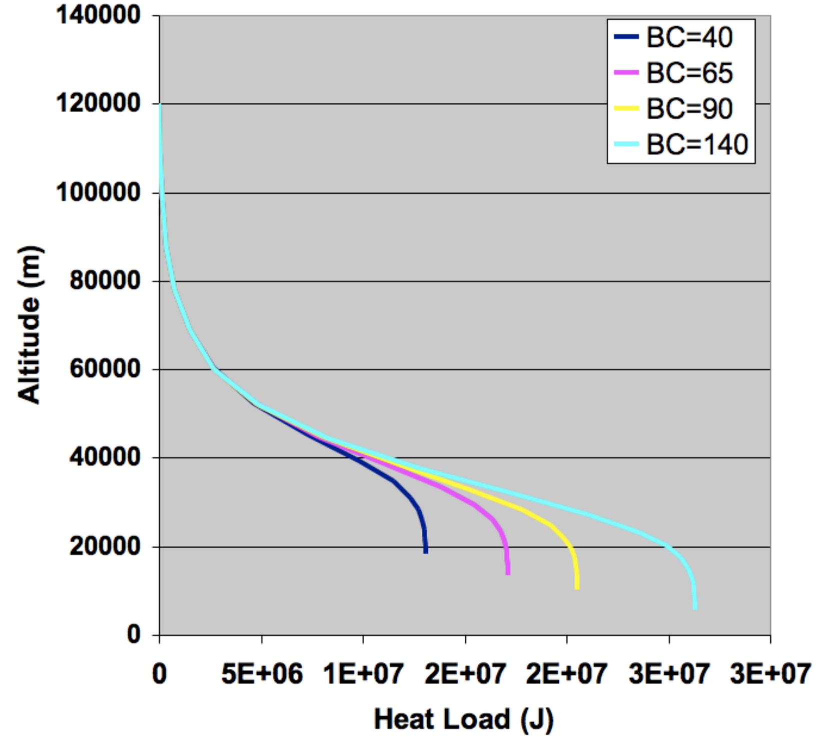

Rules of Thumb for Ballistic Entry

- Stagnation point convective heating: $q_c \sim \rho_\infty^{1/2} V_\infty^3 / R_n^{1/2}$
- Stagnation point radiative heating: $q_r \sim R_n^m$
- Wall temperature: $T_w^4 \sim q_c$
- Convective heat flux, q_c:
  - ↑ with ↑ entry velocity
  - ↑ with ↑ ballistic coefficient (mass)
  - ↑ with ↑ entry flight path angle
- Convective heat load: $Q_c = \int q_c \, dt$
  - ↑ with ↑ entry velocity
  - ↑ with ↑ ballistic coefficient (mass)
  - ↑ with ↓ entry flight path angle

Ground-to-Flight Traceability

- Ground-based testing, while valuable, cannot replicate all EDL flight conditions
  - Technically & fiscally prohibitive to build & run such facilities
- Aerodynamic heating analysis at flight conditions is usually left to engineering methods (conceptual) & high-fidelity CFD models (TPS design)
  - Ground data are used to anchor models to be used for flight predictions

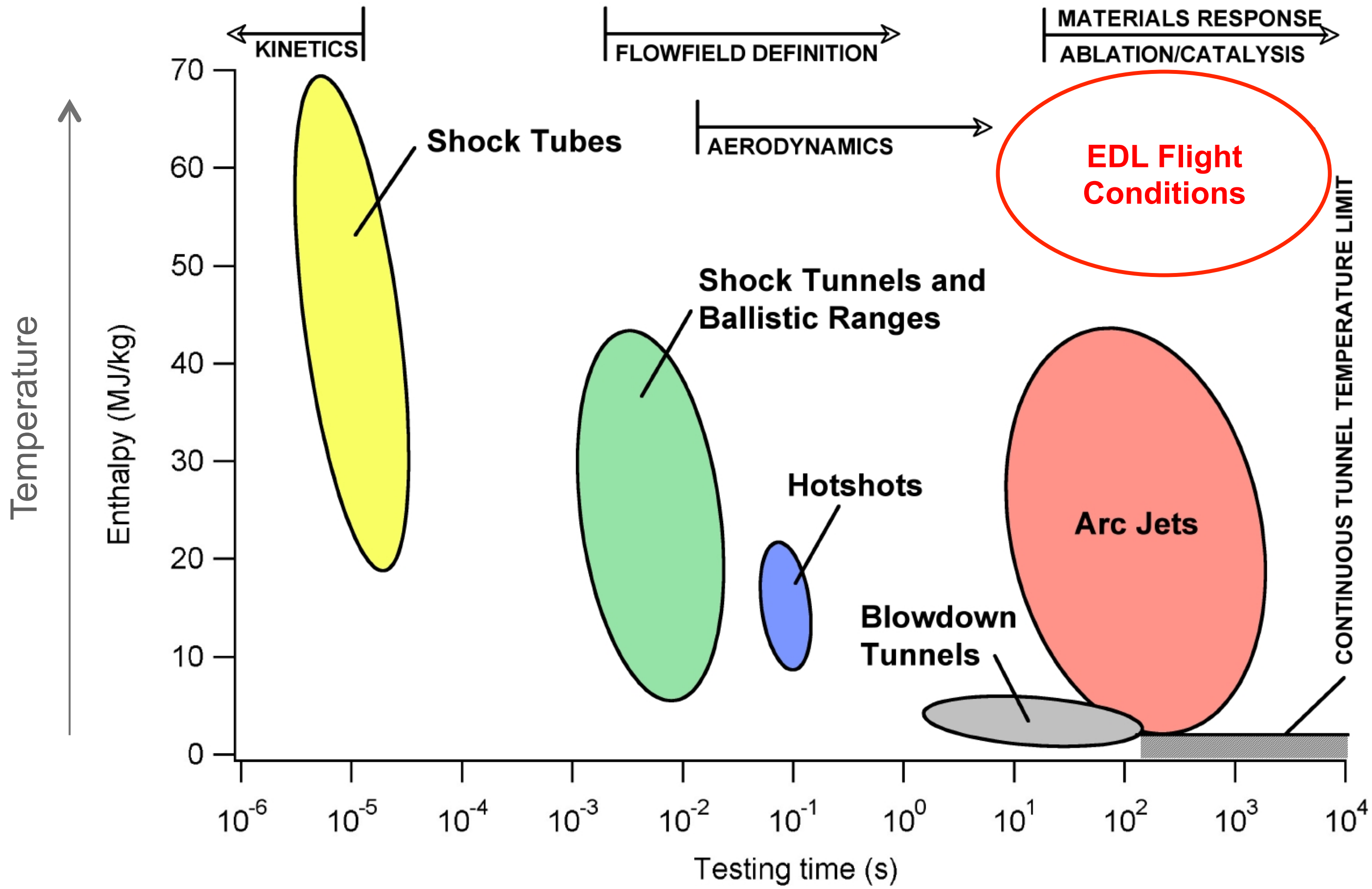

Ground-to-Flight Traceability

- Heating magnitudes in ground facilities ≠ heating in flight
  - Differences in Mach, Re, gas composition…
- Ground facilities are used to understand qualitative heating and to provide a source of data for CFD validation
  - Ground testing does not generally include TPS response, which is added post-CFD

MSL Testing in AEDC Tunnel 9 (Mach 8)

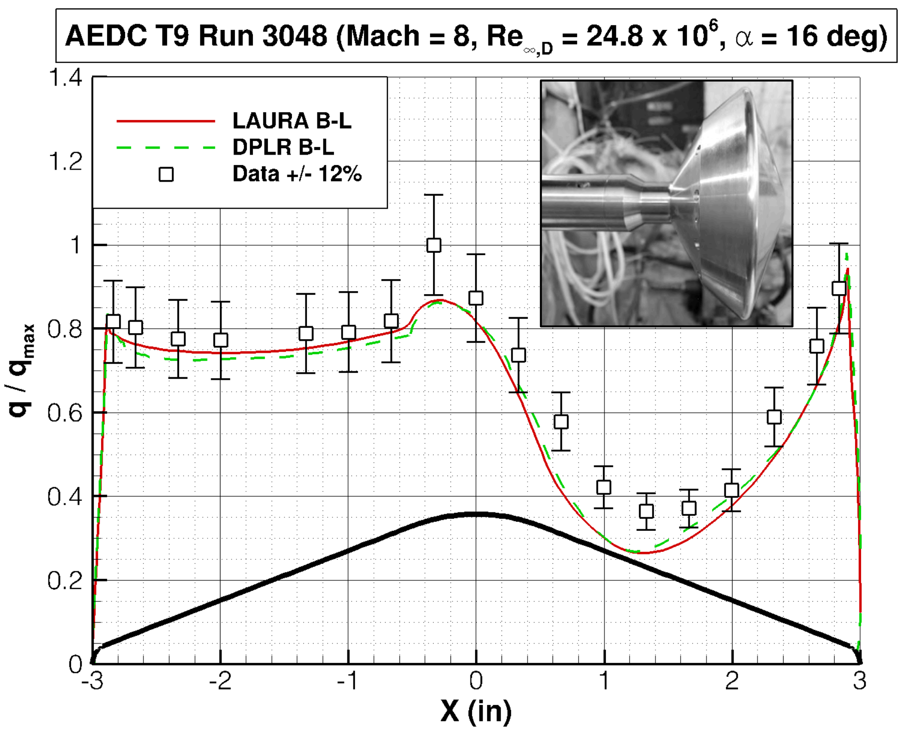

MSL Flight CFD (30 > Mach > 7)

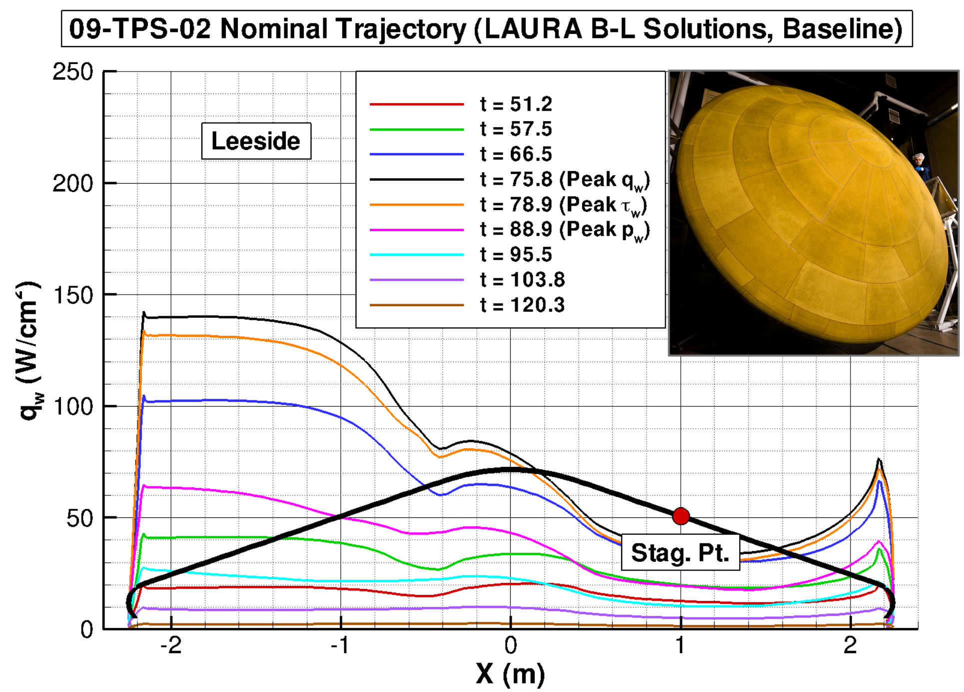

Boundary Layer Transition (BLT)

- Predicting BLT is one of the most difficult aspects of aerodynamic heating
  - Mechanisms not well understood
- BLT can increase max. heat flux and total heat load → TPS mass & performance
  - q_{Turb} > or >> q_{Lam}
  - Stagnation point may not have highest q_w
- Engineering methods are often used to predict BLT timing
  - BL momentum-thickness Reynolds no., $Re_\theta > Re_{\theta,crit}$
  - Examples: Space Shuttle, MSL
- Conservative approach is to design for turbulent conditions using CFD

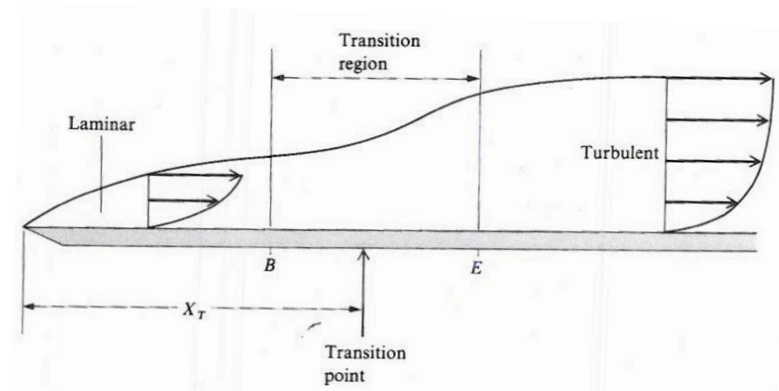

Schematic of BLT (Ref. Anderson)

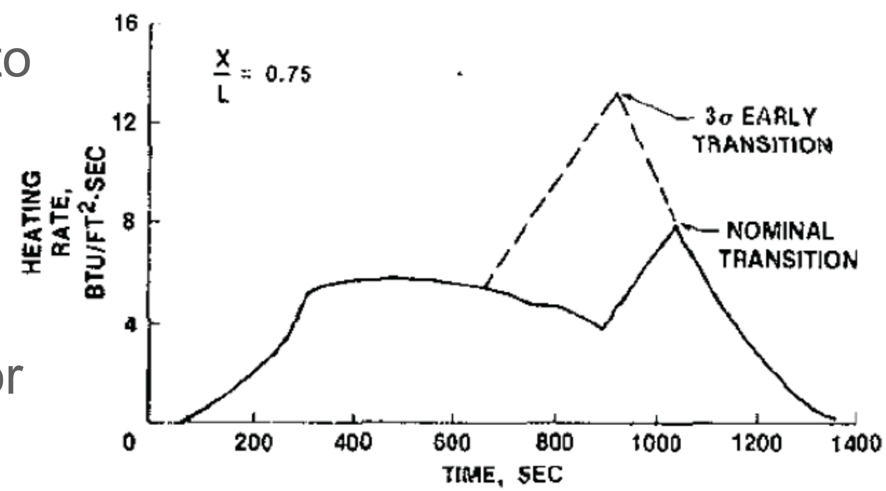

BLT Design for Space Shuttle Windward Body Point (Ref. AIAA 79-1042)

"When I meet God, I am going to ask him two questions: Why relativity? And why turbulence? I really believe he will have an answer for the first." - Werner Heisenberg

BLT on STS-119

- HYTHIRM imagery of Space Shuttle lower surface

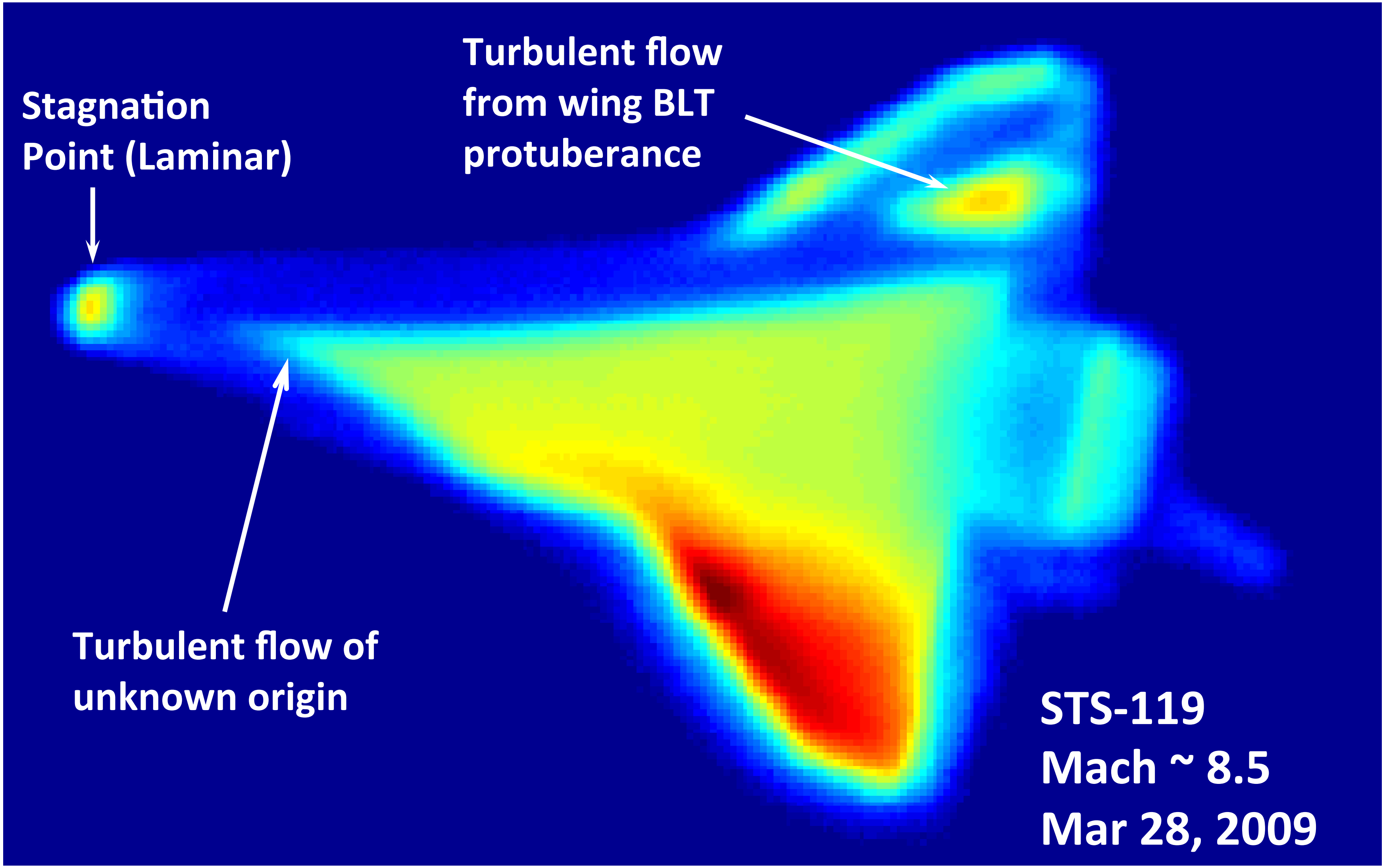

Catalytic Heating

- High shock-layer temperature dissociates gas molecules
  - Mars: CO_2/N_2 in front of shock → CO_2, N_2, O_2, CO, C, N, O behind shock
  - Earth: N_2/O_2 in front of shock → N_2, O_2, N, O, NO + ions behind shock
- Post-shock gas may recombine at surface
  - Heat of reaction = Catalytic heating = Higher convective heating
- Conservative approach is to maximize catalytic heating
  - "Super-catalytic" = recombine all atoms

Mars Non-Equilibrium Chemistry

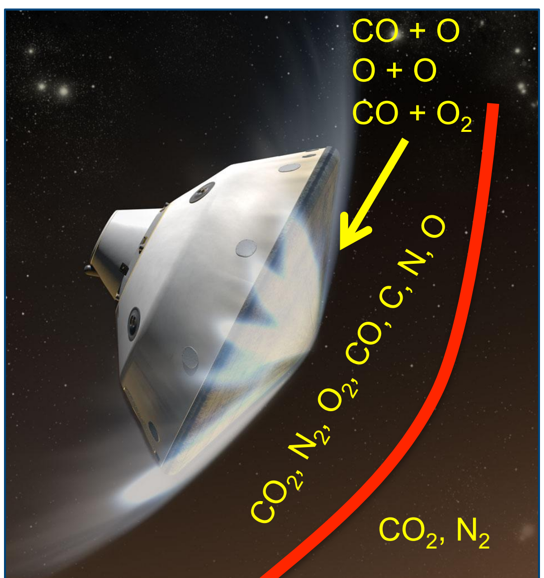

MSL Predicted Convective Heat Flux at Peak Heating (No Uncertainties)

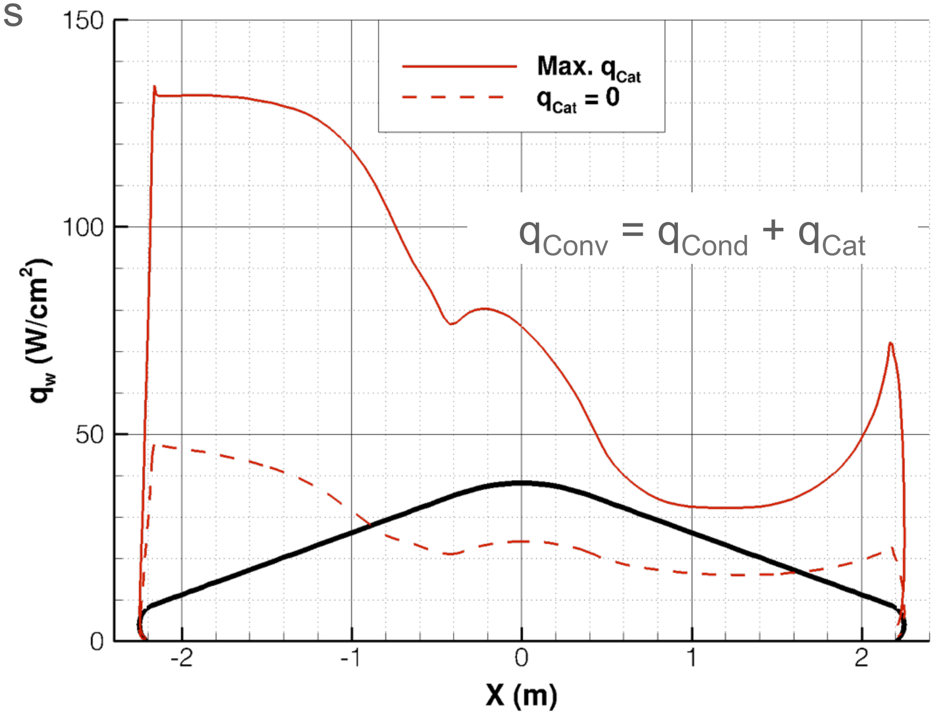

Aftbody Heating

- Heating on vehicle components that are in the wake of a hypersonic flowfield are more difficult to predict
  - Separated, unsteady, turbulent, low-density flow
  - Uncertainties are > than for heatshield
- Heating is generally < 10% of stagnation point heating for a blunt body

Ballistic Range Model

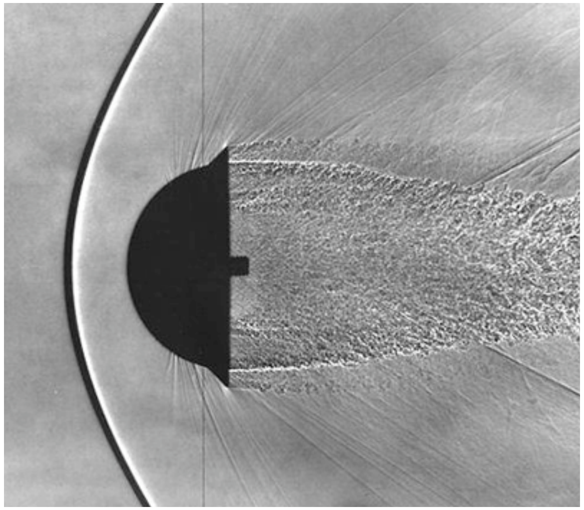

DPLR CFD of AS-202 (Ref. AIAA 2004-2456)

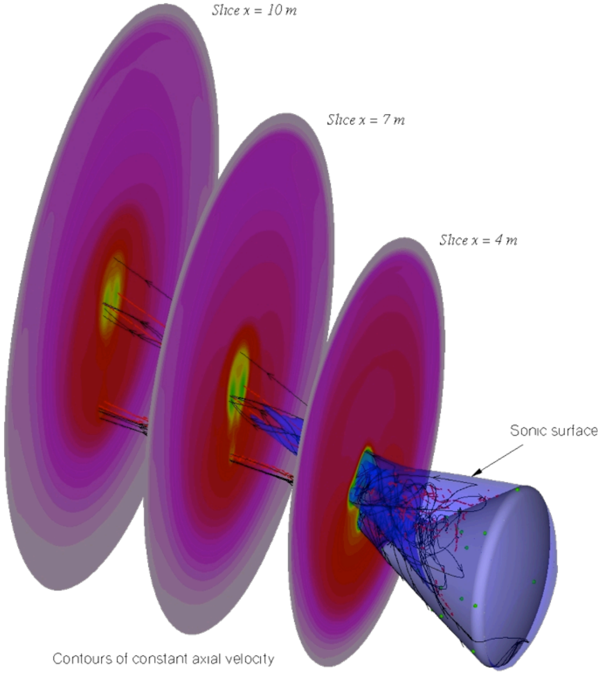

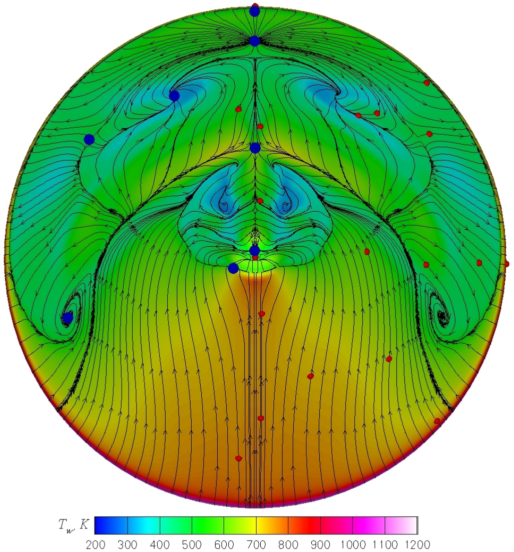

Case Study: Mars Science Laboratory

Mars Science Laboratory (MSL)

- Guided entry (trim α = -16 deg, trim L/D = 0.24), RCS bank control
- Large heatshield + high m/C_DA = BLT expected prior to peak heating, resulting in high heating rate

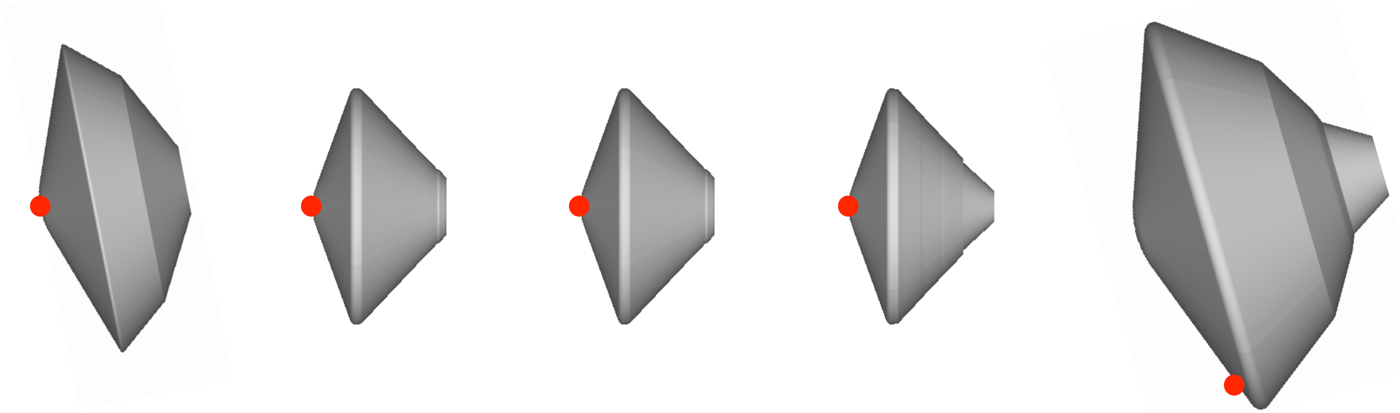

	Viking 1/2	Pathfinder	MER A/B	Phoenix	MSL
Diameter, m	**3.5**	**2.65**	**2.65**	**2.65**	**4.5**
Entry Mass, kg	**930**	**585**	**840**	**602**	**3152**
Entry Vel., km/s	**4.5/4.42**	**7.6**	**5.5**	**5.9**	**5.9**
Entry FPA, deg	**-17.6**	**-13.8**	**-11.5**	**-13**	**-16.1**
$m/(C_DA)$, kg/m^2	**64**	**62**	**90**	**65**	**135**
Hypersonic α, deg	**-11.2**	**0**	**0**	**0**	**-16**
Hypersonic L/D	**0.18**	**0**	**0**	**0**	**0.24**
Heat Flux, W/cm^2	**24**	**106**	**48**	**56**	**>200 (Design)**

MSL Heatshield & MEDLI Instrumentation

- MISP: 2-4 thermocouples (0.1-0.7 in below surface) at 7 locations
  - Surface heating comes from inverse analysis of temperature data
- MEADS: pressure transducer at 7 separate locations → capsule attitude

MEDLI Locations

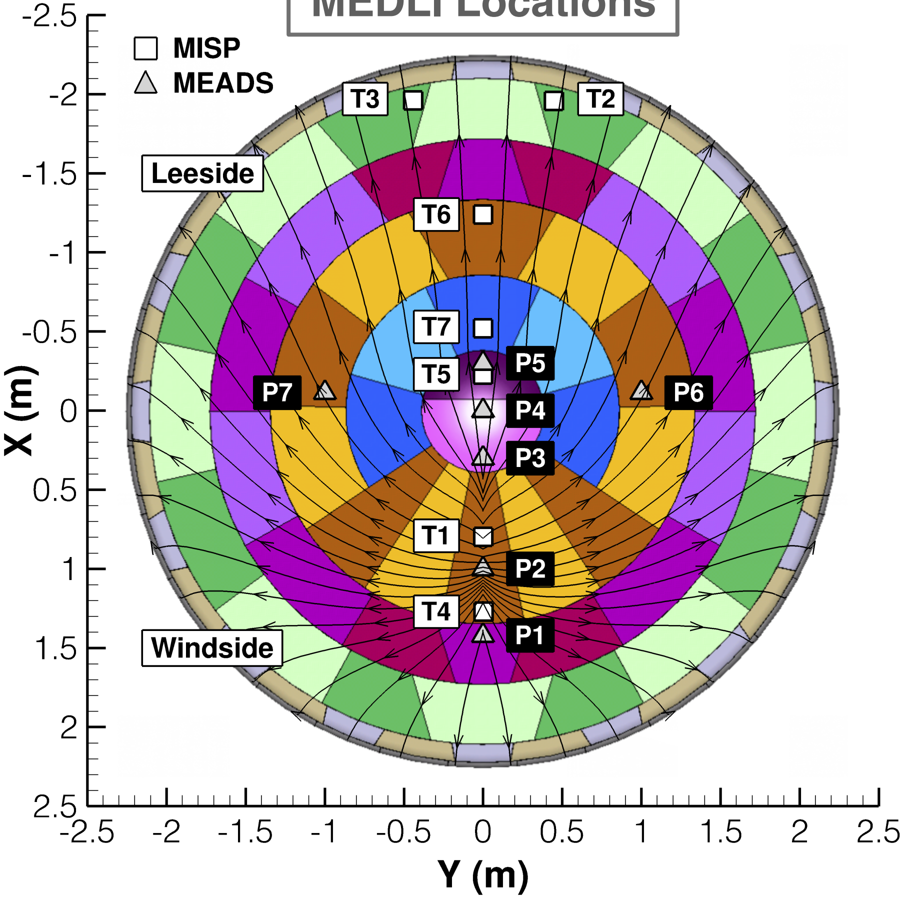

MISP Locations on Flight Heatshield

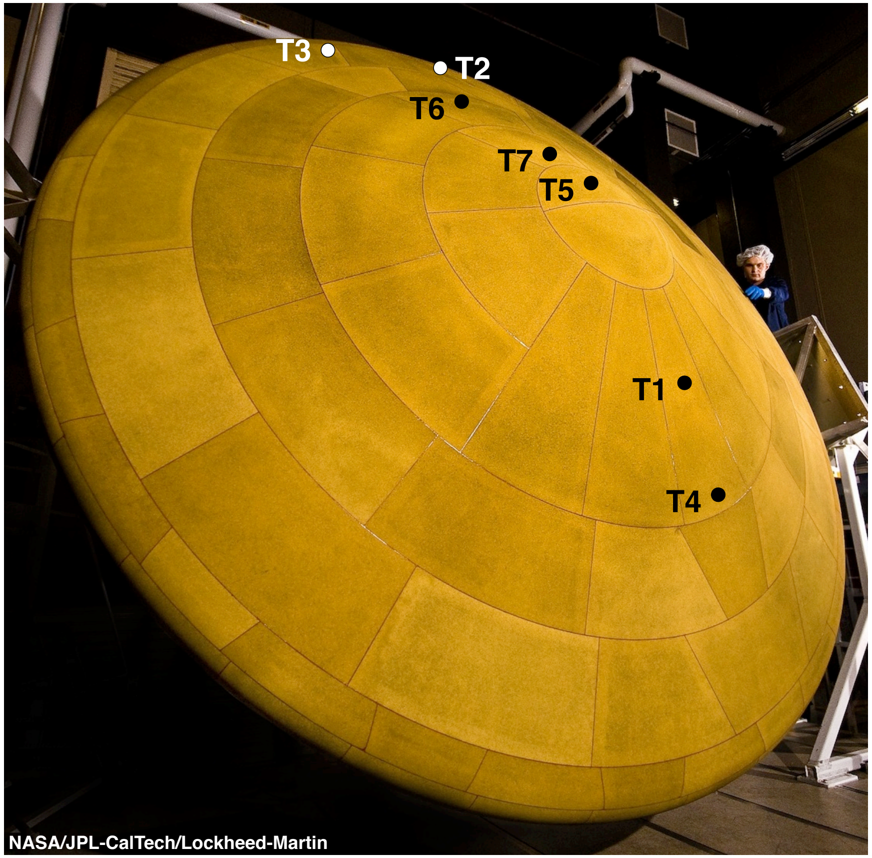

MSL Reconstructed Angle-of-Attack [28]

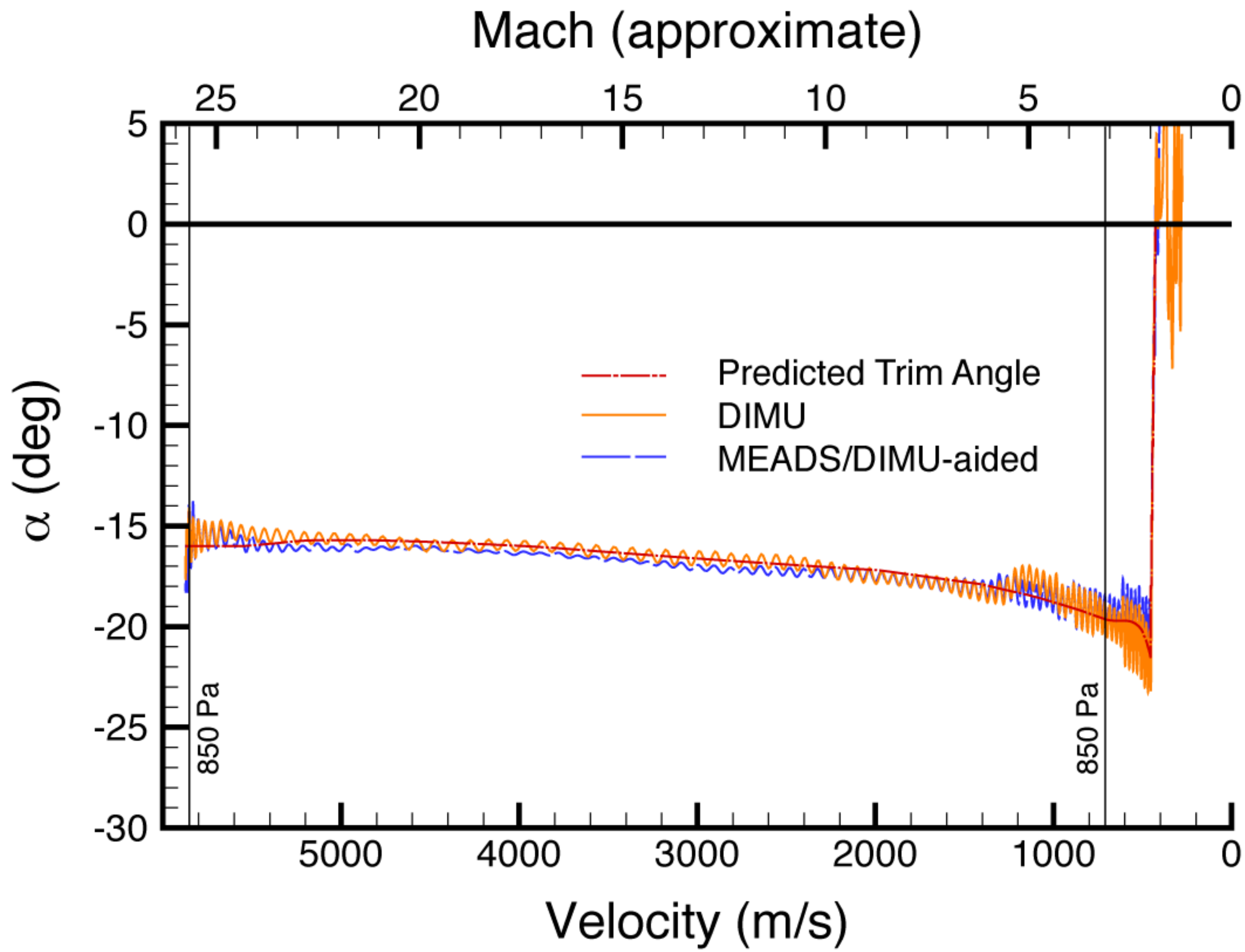

- Trim angle and Lift-to-Drag predictions were very accurate

MSL C_A [28]

$$C_A = -\frac{m_{EV} a_x}{q_{\infty,MEADS} S_{ref}}$$

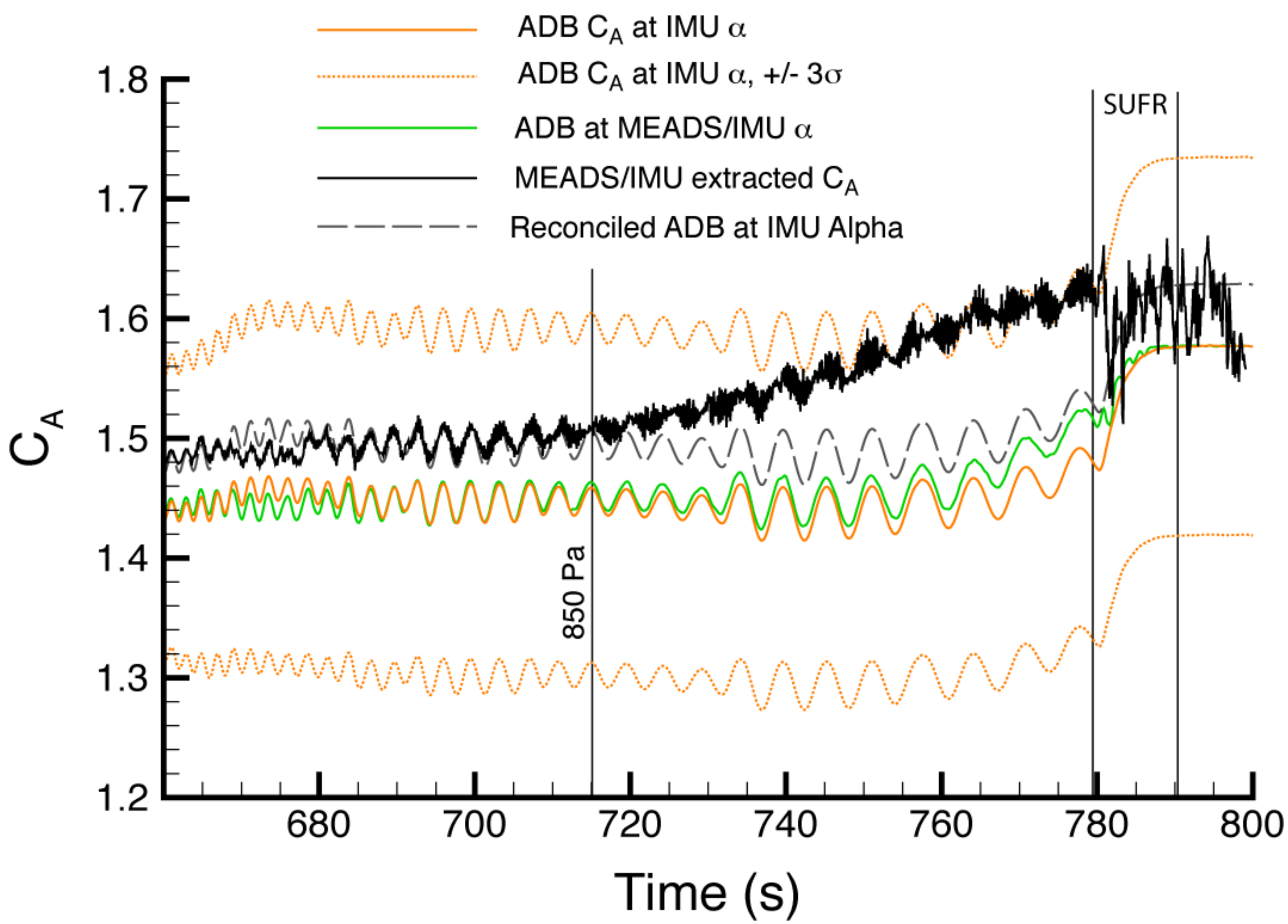

- MEADS Supersonic C_A remains area of study
- Viking-derived base pressure correction remains possible error source
- **Winds and supersonic drag are the two dominant contributors to landing miss distance**

MSL Boundary Layer Transition

- BLT indicated by rapid increase in dT/dt
- MISP T2, T3, T6, and T7 all experienced BLT
- Small bump at T5 believed to indicate BLT
- All BLT events occurred prior to peak heating, as expected

Time Rate-of-Change of Temperature 0.1 in. Below Surface

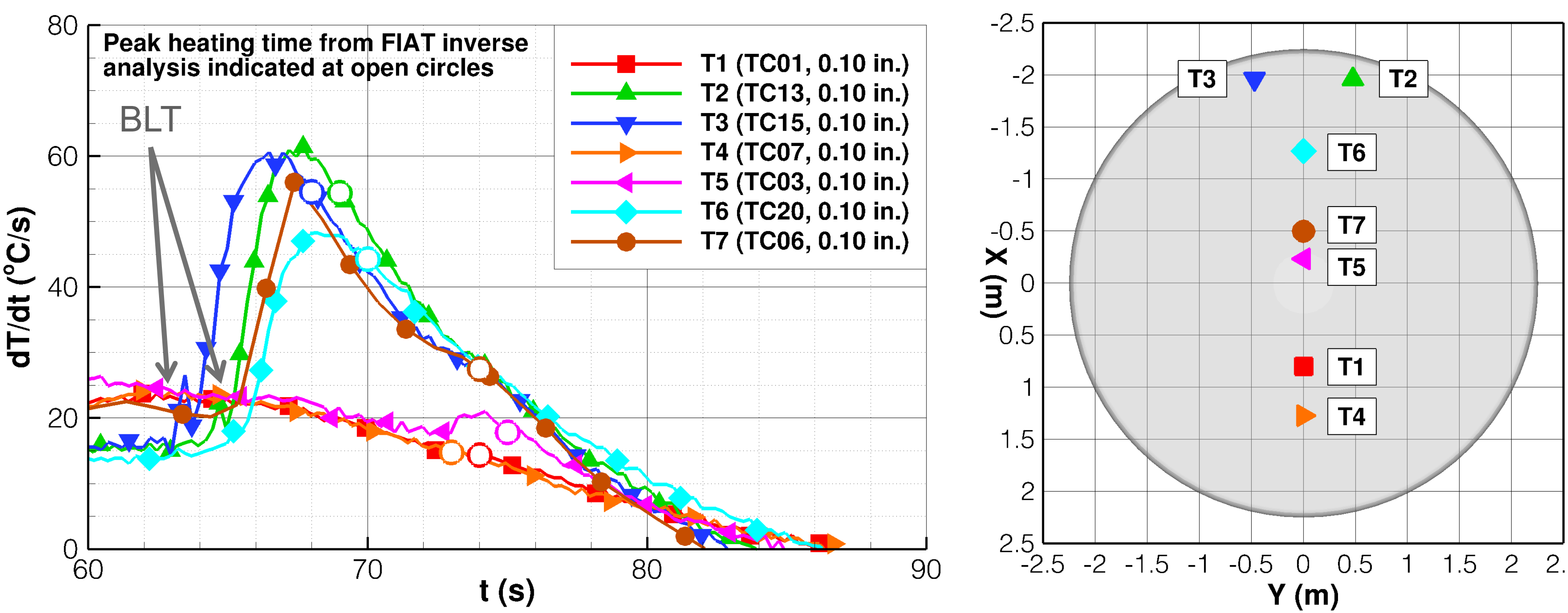

MSL Reconstructed Heating

- Expected results:
  - Laminar heating highest at T5
  - Laminar heating lowest at T2, T3, T6
  - Turbulent heating highest at T2, T3
- Unexpected results:
  - High turbulent heating at T7 relative to T2, T3 → roughness?
  - High heating at T1, T4 relative to T2, T3 → radiation?

MISP Heating Rate from FIAT Inverse Analysis (Estimated +/-15% Uncertainty)

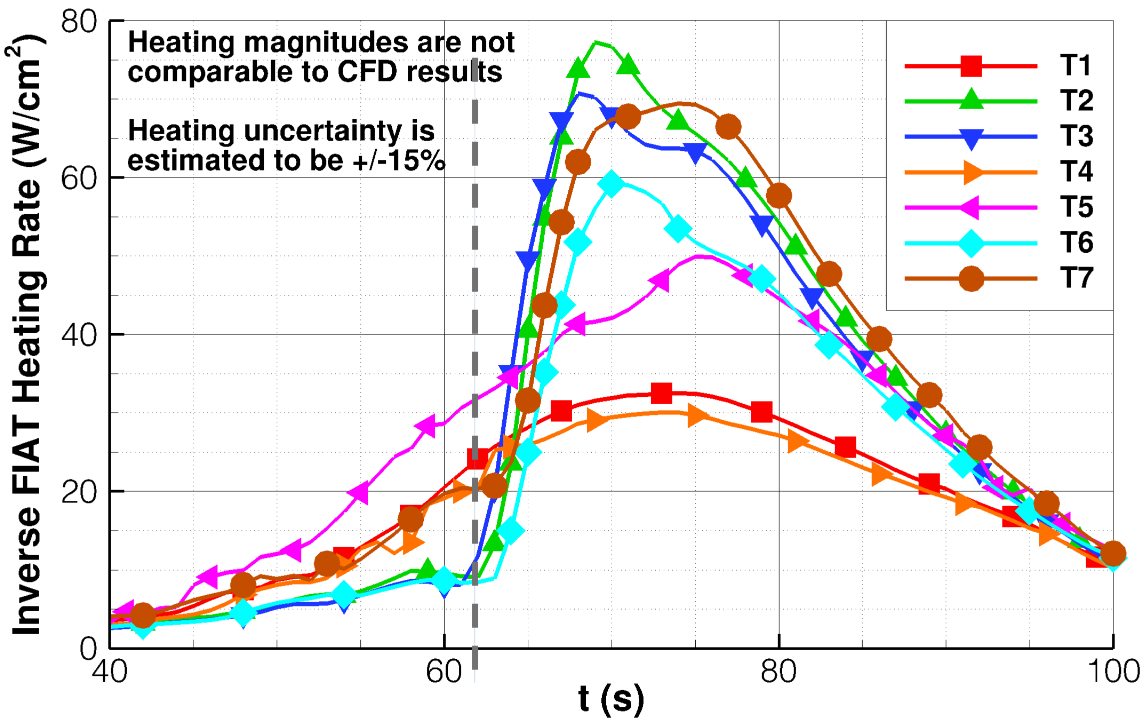

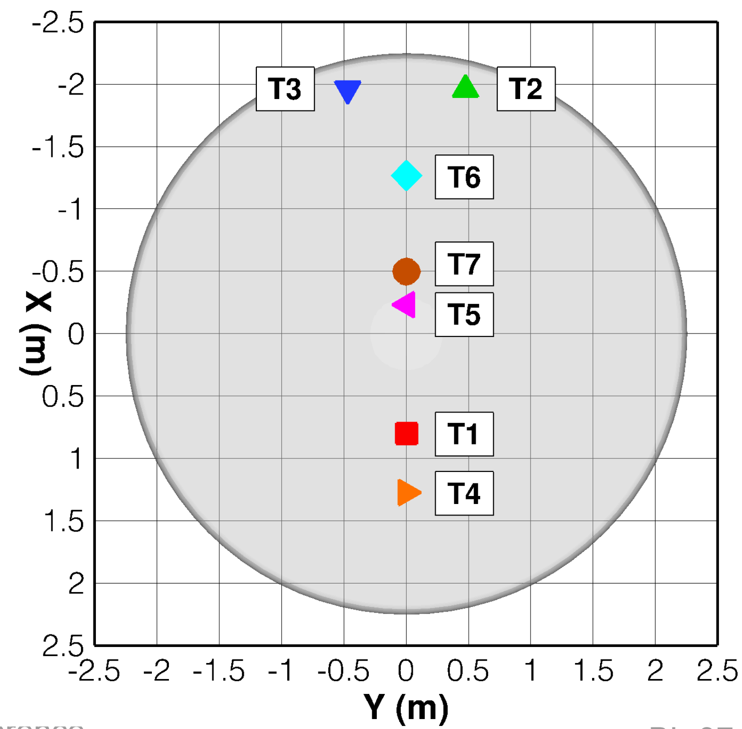

Max. Heat Flux for Select Entry Vehicles

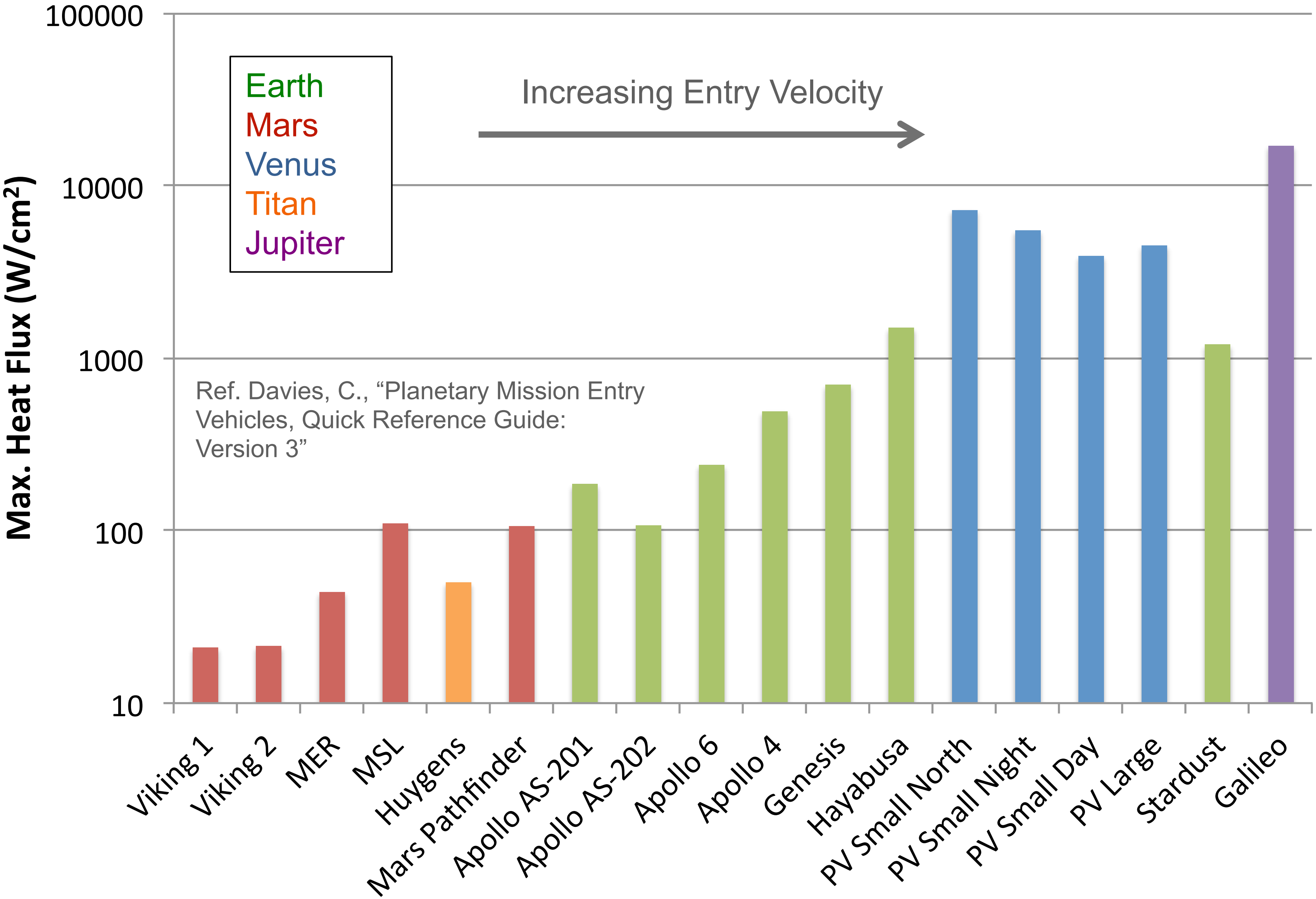

Heat Load for Select Entry Vehicles

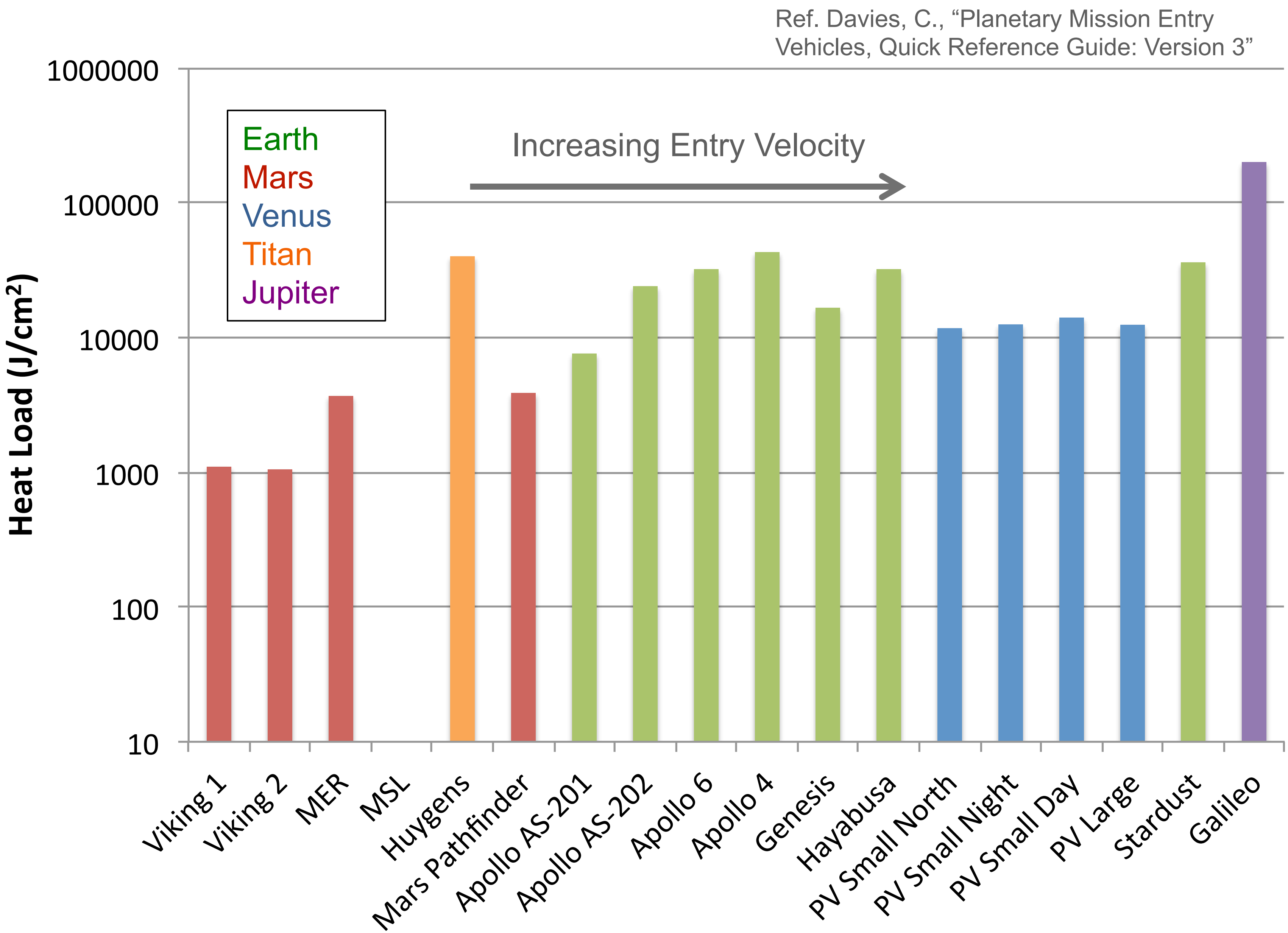

Questions/Discussion?

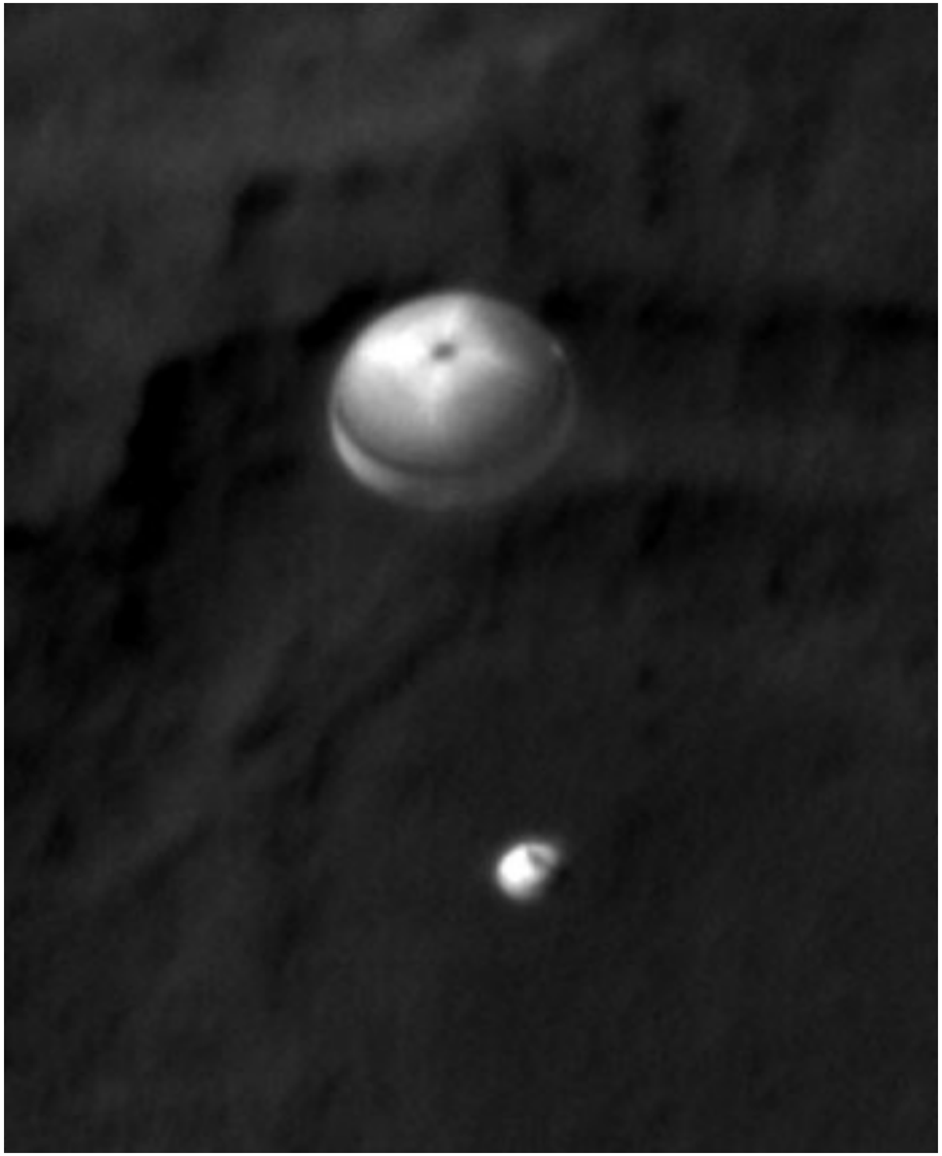

NASA/JPL-Caltech/Univ. of Arizona

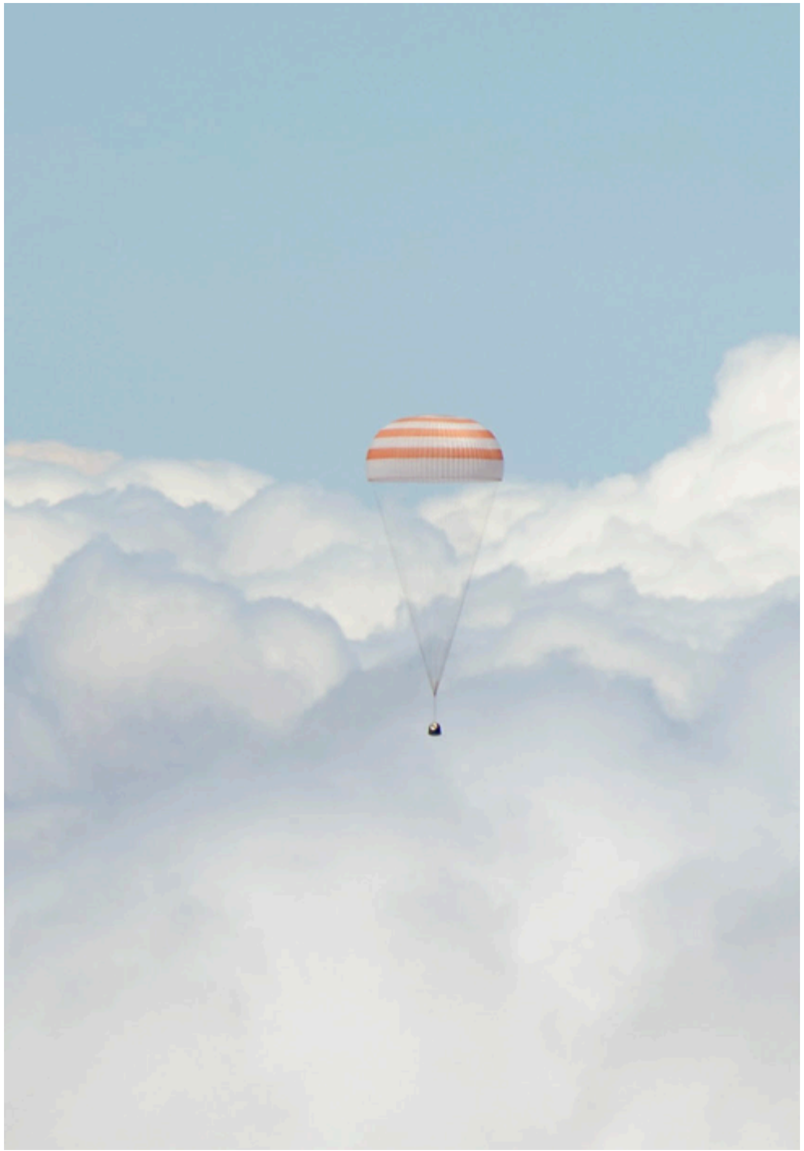

ISS Expedition 31, NASA/Bill Ingalls

Aerodynamics References

REFERENCES

Introduction

Blunt Body Aerodynamics[1]

Entry Vehicles

CORONA Aerodynamics[2–4]
- Early Manned Aerodynamics[5]
- Apollo[6–10]
- MPCV,Orion[11–14]
- Viking Aerodynamics[15–18]
- Mars Pathfinder[19–21]
- Mars Exploration Rover[22–24]
- Mars Science Laboroatory[25–28]
- Mars Phoenix[29]
- Galileo[30]
- Pioneer Venus[31]
- Microprobe[32, 33]
- Hayabusa (MUSES-C)
- Stardust[34]
- Genesis[35]
- Huygens probe[36, 37]

Static Aerodynamics

Newtonian Aerodynamics[38, 39]
- Modified Newtonian[40]
- LAURA CFD[41]
- Shape Optimization[42]
- Aerodynamic Surfaces (Trim Tabs)[43–45]

REFERENCES

Dynamic Stability

Dynamic Stability Testing[46–50]
Dynamic Stability Theory and Computation[51–56]

Reaction Control System

Reaction Control Systems[57–59]

References

[1] Allen, J. H. and Eggers, A. J. J., "A Study of the Motion and Aerodynamic Heating of Missiles Entering the Earth's Atmosphere at High Supersonic Speeds," NACA TN–4047, NACA, October 1957.

[2] Wehrend, W. R. J., "Wind-Tunnel Investigation of the Static and Dynamic Stability Characteristics of a 10 deg Semivertex Angle Blunted Cone," Tech. Rep. NASA TN D-1202, 1962.

[3] Intrieri, P. F., "Free-Flight Measurements of the Static and Dynamic Stability and Drag of a 10 deg Blunted Cone at Mach Numbers of 3.5 and 8.5," Tech. Rep. NASA TN D-1299, 1962.

[4] Treon, Stuart, L., "Static Aerodynamic Characteristics of Short Blunt Cones with Various Nose and Base Cone Angles at Mach Numbers from 0.6 to 5.5 and Angles of Attack to 180 deg," Tech. Rep. NASA TN D-1327, 1962.

[5] Sommer, S. C., Short, B. J., and Compton, D. L., "Free-Flight Measurements of Static and Dynamic Stability of Models of the Project Mercury Re-Entry Capsule at Mach Numbers 3 and 9.5," Tech. Rep. NASA TM X-373, 1960.

[6] Dodds, J. I., "Aerodynamic Data Manual for Project Apollo," SID 64- 174C, North American Aviation, Inc., 1966.

[7] Moseley, William, C., Graham, Ralph, E., and Hughes, J. E., "Aerodynamic Stablity Characteristics of the Apollo Command Module," Tech. Rep. NASA TN D-4688, 1967.

[8] Averett, B. T., "Dynamic-Stability Characteristics in Pitch of Models of Proposed Apollo Configurations at Mach Numbers from 0.30 to 4.63," Tech. Rep. NASA TM X-1127, 1965.

[9] Moseley, William C.Jr.and Moore, R. H. J. and Hughes, J. E., "Stability Characteristics of the Apollo Command Module," Tech. Rep. NASA TN D-3890, 1967.

[10] Moseley, William C.Jr.and Martino, J. C., "Apollo Wind Tunnel Testing Program - Historical Development of General Configurations," Tech. Rep. NASA TN D-3748, 1966.

[11] Murphy, K. J., Borg, S. E., Watkins, A. N., Cole, D. R., and Schwartz, R. J., "Testing of the Crew Exploration Vehicle in NASA Langley's Unitary Plan Wind Tunnel," AIAA 2007-1005, 2007.

[12] Murphy, K. J., Bibb, K. L., Brauckmann, G. J., Rhode, Matthew, N., Owens, B., Chan, D. T., and Walker, E. L., "Orion Crew Module Aerodynamic Testing," AIAA 2011-3502, 2011.

[13] Bibb, K. L., Walker, E. L., Brauckmann, G. J., and E., R. P., "Development of the Orion Crew Module Static Aerodynamic Database, Part I: Hypersonic," AIAA 2011-3506, 2011.

REFERENCES

[14]Bibb, K. L., Walker, E. L., Brauckmann, G. J., and E., R. P., "Development of the Orion Crew Module Static Aerodynamic Database, Part II: Supersonic/Subsonic," AIAA 2011-3507, 2011.

[15]Flaherty, T. M., "Aerodynamics Data Book," TR- 3709014, Martin Marietta Corporation, 1972.

[16]Steinberg, S., "Experimental Pitch Damping Derivatives for Candidate Viking Entry Configurations at Mach Numbers from 0.6 Through 3.0," TR- 3709005, Martin Marietta Corporation, June 1970.

[17]Ingoldby, R. N., Michel, F. C., Flaherty, T. M., Doty, M. G., Preston, B., Villyard, K. W., and Steele, R. D., "Entry Data Analysis for Viking Landers 1 and 2," TN- 3770218, Martin Marietta Corporation, 1976.

[18]Holmberg, N. A. and Faust, R. P., "Viking '75 Spacecraft Design and Test Summary, Volume 1 - Lander Design," NASA Reference Publication 1027, 1980.

[19]Gnoffo, P. A., Braun, R. D., Weilmuenster, J. K., Mitcheltree, R. A., Engelund, W. C., and Powell, R. W., "Prediction and Validation of Mars Pathfinder Hypersonic Aerodynamic Database," *Journal of Spacecraft and Rockets*, Vol. 36, No. 3, May-June 1999, pp. 367–373.

[20]Braun, R. D., Powell, R. W., Engelund, W. C., C., G. P., Weilmuenster, J. K., and Mitcheltree, R. A., "Mars Pathfinder Six-Degree-of-Freedom Entry Analysis," *Journal of Spacecraft and Rockets*, Vol. 32, No. 6, pp. 993–1000.

[21]Spencer, D. A., Blanchard, R. C., Braun, R. D., Kallemeyn, P. H., and Thurman, S. W., "Mars Pathfinder Entry, Descent, and Landing Reconstruction," *Journal of Spacecraft and Rockets*, Vol. 36, No. 3, May-June 1999, pp. 357–366.

[22]Desai, P. N., Schoenenberger, M., and Cheatwood, F. M., "Mars Exploration Rover Six-Degree-of-Freedom Entry Trajectory Analysis," AAS 03-642, August 2003.

[23]Schoenenberger, M., Cheatwood, F., and Desai, P., "Static Aerodynamics of the Mars Exploration Rover Entry Capsule," AIAA 2005–0056, January 2005.

[24]Schoenenberger, M., Hathaway, W., Yates, L., and Desai, P., "Ballistic Range Testing of the Mars Exploration Rover Entry Capsule," AIAA 2005–0055, January 2005.

[25]Dyakonov, A. A., Schoenenberger, M., and Van Norman, J. W., "Hypersonic and Supersonic Static Aerodynamics of Mars Science Laboratory Entry Vehicle," AIAA 2012-2999, 2012.

[26]Schoenenberger, M., Dyakonov, A., Buning, P., Scallion, W., and Van Norman, J., "Aerodynamic Challenges for the Mars Science Laboratory Entry, Descent and Landing," AIAA 2009-3914, 2009.

[27]Schoenenberger, M., Yates, L., and Hathaway, W., "Dynamic Stability Testing of the Mars Science Laboratory Entry Capsule," AIAA 2009-3917, 2009.

[28]Schoenenberger, M., Van Norman, J., Dyakonov, A., Karlgaard, C., Way, D., and Kutty, P., "Assessment of the Reconstructed Aerodynamics of the Mars Science Laboratory Entry Vehicle," AAS 13-306, 2013.

[29]Desai, P. N., Prince, J. L., Queen, E. M., and Cruz, J. R., "Entry, Descent and Landing Performance of the Mars Phoenix Lander," AIAA 2008-7346, 2008.

[30]Intrieri, P. F. and Kirk, D. B., "High-Speed Aerodynamics of Several Blunt-Cone Configurations," *Journal of Spacecraft*, Vol. 24, No. 2, March-April 1987, pp. 127–132.

[31]Intrieri, P. F., DeRose, C. E., and Kirk, D. B., "Flight Characteristics of Probes in the Atmospheres of Mars, Venus and the Outer Planets," *Acta Astronautica*, Vol. 4, July-August 1977, pp. 789–799.

[32]Mitcheltree, R. A., Moss, J. N., Cheatwood, F. M., Greene, F. A., and Braun, R. D., "Aerodynamics of the Mars Microprobe Entry Vehicles," AIAA 1997-3658, 1997.

[33]Braun, R. D., Mitcheltree, R. A., and Cheatwood, F. M., "Mars Microprobe Entry-to-Impact Analysis," *Journal of Spacecraft and Rockets*, Vol. 36, No. 3, May-June 1999, pp. 412–420.

[34]Chapman, G. T., Mitcheltree, R. A., and Hathaway, W. H., "Transonic and Low Supersonic Static and Dyanmic Aerodynamic Characteristics of the Stardust Sample Return Capsule," AIAA 99-1021, 1999.

REFERENCES

[35]Cheatwood, F., Winchenbach, G., Hathaway, W., and Chapman, G., "Dynamic Stability Testing of the Genesis Sample Return Capsule," AIAA 2000–1009, January 2000.

[36]Chapman, G. T. and Yates, Leslie, A., "Dynamics of Planetary Probes: Design and Testing Issues," AIAA 1998–0797, 1998.

[37]Winchenbach, G. L., Hathaway, W. H., Chapman, G. T., Berner, C., and Ramsey, A., "The Dynamic Stability of Blunt Atmospheric Entry Configurations," AIAA 2000–4115, 2000.

[38]von Karman, T., "Isaac Newton and Aerodynamics," *Journal of the Aeronautical Sciences*, Vol. 9, No. 14, December 1942, pp. 521–522,548.

[39]Anderson, J. D. J., *Hypersonic and High Temperature Gas Dynamics*, McGraw-Hill, New York, 1989.

[40]Lees, L., "Hypersonic Flow," *Fifth International Aeronautical Conference, Los Angeles*, 1955, pp. 247–276.

[41]Cheatwood, F. M. and Gnoffo, P. A., "User's Manual for the Langley Aerothermodynamic Upwind Relaxation Algorithm (LAURA)," NASA TM 4674, 1996.

[42]Theisinger, J. E. and Braun, R. D., "Multi-Objective Hypervelocity Entry Aeroshelll Shape Optimization," *Journal of Spacecraft and Rockets*, Vol. 46, No. 5, September-October 2009, pp. 957–966.

[43]Lockwood, M. K., Sutton, K., Prabhu, R., Powell, R. W., Graves, C. A., Epp, C., and Carman, G., "Entry Configurations and Performanc Comparisons for the Mars Smart Lander," AIAA 2002-4407, 2002.

[44]Horvath, T. J., O'Connell, T. F., Cheatwood, F. M., and Alter, S. J., "Experimental Hypervelocity Aerodynamic Characteristics of the Mars Surveyor 2001 Precision Lander with Deployable Flap," AIAA 2002-4408, 2002.

[45]Brown, J., Yates, L., Bogdanoff, D., Chapman, G., Loomis, M., and Tam, T., "Free Fligth Testing in Support of the Mars Smart Lander Aerodynamics Database," AIAA 2002-4410, 2002.

[46]Schueler, C. J., Ward, L. K., and Hodapp, A. E. J., "Techniques for Measurement of Dynamic Stability Derivatives in Ground Test Facilities," AGARDograph 121, 1967.

[47]Winchenbach, G. L., "Aerodynamic Testing in a Free-Flight Spark Range," Tech. Rep. WL-TR-1997-7006, Wright Laboratory, Armament Directorate, Weapon Flight Mechanics Division (WL/MNAV), Eglin AFB, FL, April 1997.

[48]Hathaway, W. H. and Whyte, R. H., "Aeroballistic Research Facility Free Flight Data Analysis Using Maximum Likelihood Method," AFATL-TR -79-98, Air Force Armament Laboratory, Eglin AFB, FL, December 1979.

[49]Yates, L. A., "A Comprehensive Aerodynamic Data Reduction System for Aeroballistic Ranges," WL-TR -96-7059, Wright Laboratory, Eglin AFB, FL, October 1996.

[50]Braslow, A. L., Harleth, G. W., and Cullen, Q. L., "A Rigidly Forced Oscillation System for Measuring Dynamic-Stability Parameters in Transonic and Supersonic Wind Tunnels," Tech. Rep. NASA TN D-1231, 1962.

[51]Tobak, M. and Wehrend, W. R., "Stability Derivatives for Cones at Supersonic Speeds," NACA TN–3788, NACA, September 1956.

[52]Redd, B., Olsen, D. M., and Barton, R. L., "Relationship Between the Aerodynamic Damping Derivatives Measured as a Function of Instantaneous Angular Displacement and the Aerodynamic Damping Derivatives Measured as a Function of Oscillation Amplitude," Tech. Rep. NASA TN D-2855, 1965.

[53]Chapman, G. T. and Yates, L. A., "Limit Cycle Analysis of Blunt Entry Vehicles," AIAA 99–1022, January 1999.

[54]Schoenenberger, M., Queen, E. M., and Litton, D., "Oscillation Amplitude Growth for a Decelerating Object with Constant Pitch Damping," AIAA 2006–6148, 2006.

[55]Schoenenberger, M. and Queen, E. M., "Limit Cycle Analysis Applied to the Oscillations of Decelerating Blunt-Body Entry Vehicles," NATO RTO-MP-AVT-152-006, 2008.

REFERENCES

[56]Teramoto, S., Hiraki, K., and Fugii, K., "Numerical Analysis of Dynamic Stability of a Reentry Capsule at Transonic Speeds," *AIAA Journal*, Vol. 39, No. 4, April 2001, pp. 646–653.

[57]Dyakonov, A. A., Schoenenberger, M., Scallion, W. I., Van Norman, J., Novak, L., and Tang, C., "Aerodynamic Interference Due to MSL Reaction Control System," AIAA 2009-3915, 2009.

[58]Schoenenberger, M., Van Norman, J., Rhode, M., and Paulson, J., "Characterization of Aerodynamic Interactions with the Mars Science Laboratory Reaction Control System Using Computation and Experiment," AIAA 2013-0971, 2013.

[59]Johansen, C., Danehy, P., Ashcraft, S., Bathel, B., Inman, J., and Jones, S., "PLIF Study of Mars Science Laboratory Capsule Reaction Control System Jets," AIAA 2011-3890, 2011.

Aerothermodynamics References

References

Theory, Engineering Methods, History

1. Anderson, John D., Jr., *Hypersonic and High Temperature Gas Dynamics*, McGraw-Hill Series in Aeronautical and Aerospace Engineering, 1989.
2. Anderson, John D., Jr., *Modern Compressible Flow: With Historical Perspective*, 2nd Edition, McGraw-Hill Series in Aeronautical and Aerospace Engineering, 1990.
3. Lees, L. “Laminar Heat Transfer Over Blunt-Nosed Bodies at Hypersonic Speeds,” *Jet Propulsion*, pp. 256-269, Apr. 1956
4. Allen, H. J. and Eggers, Jr., A. J., "A Study of the Motion and Aerodynamic Heating of Ballistic Missiles Entering the Earth's Atmosphere at High Supersonic Speeds,” NACA Annual Report (NASA Technical Reports) 44.2 (NACA-TR-1381), 1958
5. Fay, J.A. and Riddell, F.R., “Theory of Stagnation Point Heat Transfer in Dissociated Air,” *Journal of Aeronautical Sciences*, Feb. 1958
6. Chapman, G.T., “Theoretical Laminar Convective Heat Transfer & Boundary Layer Characteristics on Cones at Speeds to 24 km/s,” NASA TN D-2463, 1964
7. Sutton, K. and Graves, R.A., “A General Stagnation Point Convective Heating Equation for Arbitrary Gas Mixtures,” NASA TR- R-376, 1971
8. Tauber, M., “A Review of High-Speed, Convective Heat Transfer Computation Methods,” NASA TP-2914, Jul. 1989.
9. Davies, C., “Planetary Mission Entry Vehicles, Quick Reference Guide: Version 3,” NASA/SP-2006-3401, NASA Ames Research Center, Space Technology Division

References

CFD

1. Cheatwood, F. M. and Gnoffo, P. A., “Users Manual for the Langley Aerothermodynamic Upwind Algorithm (LAURA),” NASA TM-4674, April 1996.
2. Wright, M. J., Candler, G. V., and Bose, D., “Data-Parallel Line Relaxation Method for the Navier-Stokes Equations,” AIAA Journal, Vol. 36, No. 9, 1998, pp. 1603-1609.
3. Wright, M. J., Edquist, K. T., Hollis, B. R., Olejniczak, J., and Venkatapathy, E., “Status of Aerothermal Modeling for Current and Future Mars Exploration Missions," IEEEAC Paper 1428, IEEE Aerospace Conference, Big Sky, Montana, March 2006.

References

Mars

1. Wright, M. J., Edquist, K. T., Hollis, B. R., Olejniczak, J., and Venkatapathy, E., "Status of Aerothermal Modeling for Current and Future Mars Exploration Missions," IEEEAC Paper 1428, IEEE Aerospace Conference, Big Sky, Montana, March 2006.
2. Edquist, K. T., Dyakonov, A. A., Wright, M. J., and Tang, C.-Y., “Aerothermodynamic Design of the Mars Science Laboratory Heatshield,” AIAA Paper 2009-4075, AIAA Thermophysics Conference, San Antonio, Texas, June 2009.
3. Edquist, K. T., Dyakonov, A. A., Wright, M. J., and Tang, C.-Y., “Aerothermodynamic Design of the Mars Science Laboratory Backshell and Parachute Cone," AIAA Paper 2009-4078, AIAA Thermophysics Conference, San Antonio, Texas, June 2009.
4. Hollis, B. R., and Collier, A. S., “Turbulent Aeroheating Testing of Mars Science Laboratory Entry Vehicle,” Journal of Spacecraft and Rockets, Vol. 45, No. 3, May-June 2008, pp. 417-427.
5. Tang, C., Edquist, K. T., Wright, M. J., Sepka, S., and Cassel, A., “Numerical Simulations of Protruding Gapfillers on the Mars Science Laboratory Heatshield," AIAA Paper 2009-4077, AIAA Thermophysics Conference, San Antonio, Texas, June 2009.
6. Wright, M. J., Olejniczak, J., Brown, J. L., Hornung, H. G., and Edquist, K. T., “Computational Modeling of T5 Laminar and Turbulent Heating Data on Blunt Cones, Part 2: Mars Applications," AIAA Paper 2005-0177, AIAA Aerospace Sciences Meeting and Exhibit, Reno, Nevada, January 2005.

References

Ablative TPS, Instrumentation

1. Beck, R. A. S., et al, “Development of the Mars Science Laboratory Heatshield Thermal Protection System," AIAA Paper 2009-4229, AIAA Thermophysics Conference, San Antonio, Texas, June 2009.
2. Wright, M., Beck, R., Edquist, K., Driver, D., Sepka, S., and Slimko, E., “Sizing and Margins Assessment of the Mars Science Laboratory Aeroshell Thermal Protection System," AIAA Paper 2009-4231, AIAA Thermophysics Conference, San Antonio, Texas, June 2009.
3. Gazaric, M., Wright, M., Little, A., Cheatwood, F. M., Herath, J., Munk, M., Novak, F., and Martinez, E., “Overview of the MEDLI Project," IEEE Paper 2008-1510, IEEE Aerospace Conference, Big Sky, Montana, March 2008.
4. Tran, H., Johnson, C. E., Rasky, D. J., Hui, F. C., Hsu, M.-T., Chen, T., Chen, Y.-K., Paragas, D., and Kobayashi, L., “Phenolic Impregnated Carbon Ablators (PICA) as Thermal Protection Systems for Discovery Missions," NASA TM-110440, April 1997.
5. Olynick, D., Chen, Y.-K, and Tauber, M. E., “Forebody TPS Sizing with Radiation and Ablation for the Stardust Sample Return Capsule," AIAA-972474, AIAA Thermophysics Conference, Atlanta, Georgia, June, 1997.
6. Willcockson, W. H., “Mars Pathfinder Heatshield Design and Flight Experience," Journal of Spacecraft and Rockets, Vol. 36, No. 3, May-June 1999.

References

MSL

1. Edquist, K. T., Dyakonov, A. A., Wright, M. J., Tang, C.-Y., “Aerothermodynamic Design of the Mars Science Laboratory Heatshield,” AIAA Paper 2009-4075, AIAA Thermophysics Conference, San Antonio, Texas, 22 - 25 June 2009.
2. Edquist, K., Hollis, B, Johnston, C., Bose, D., White, T., Mahzari, M., "Mars Science Laboratory Heatshield Aerothermodynamics: Design and Reconstruction," AIAA Paper 2013-XXXX, AIAA Thermophysics Conference, San Diego, California, 24 - 27 June 2013.
3. Mahzari, M., Braun, R., White, T., Bose, D., "Preliminary Analysis of the Mars Science Laboratory's Entry Aerothermodynamic Environment and Thermal Protection System Performance," AIAA Paper 2013-0185, AIAA Aerospace Sciences Meeting, Grapevine, Texas, 7 - 10 January 2013.
4. Bose, D., White, T., Santos, J., Feldman, J., Mahzari, M., Olson, M., Laub, B., "Initial Assessment of Mars Science Laboratory Heatshield Instrumentation and Flight Data," AIAA Paper 2013-908, AIAA Aerospace Sciences Meeting, Grapevine, Texas, 7 - 10 January 2013.
5. Bose, D., White, T., Santos, J., Feldman, J., Mahzari, M., Edquist, K., "A Reconstruction of Aerothermal Environment and Thermal Protection System Response of the Mars Science Laboratory Entry Vehicle," AAS Paper 13-311, AAS/AIAA Spaceflight Mechanics Meeting, Kauai, Hawaii, 10 - 14 February 2013.
6. Bose, D., White, T., Feldman, J., Santos, J., Mahzari, M., "Mars Science Laboratory Heat Shield Instrumentation and Post-Flight Analyses," AIAA Paper 2013-XXXX, AIAA Thermophysics Conference, San Diego, California, 24 - 27 June 2013.
7. White, T., Mahzari, M., Bose, D., Santos, J., "Postflight Analysis of Mars Science Laboratory's Entry Aerothermal Environment and Thermal Protection System Response," AIAA Paper 2013-XXXX, AIAA Thermophysics Conference, San Diego, California, 24 - 27 June 2013.
8. Mahzari, M., White, T., Braun, R., Bose, D., "Inverse Estimation of Mars Science Laboratorys Entry Aerothermal Environment and Thermal Protection System Response," AIAA Paper 2013-XXXX, AIAA Thermophysics Conference, San Diego, California, 24 - 27 June 2013.
9. Karlgaard, C., Kutty, P., Schoenenberger, M., Shidner, J., Munk, M., "Mars Entry Atmospheric Data System Trajectory Reconstruction Algorithms and Flight Results," AIAA Paper 2013-0028, AIAA Aerospace Sciences Meeting, Grapevine, Texas, 7 - 10 January 2013.
10. Karlgaard, C., Schoenenberger, M., Kutty, P., Shidner, J., "Mars Science Laboratory Entry, Descent, and Landing Trajectory and Atmosphere Reconstruction," AAS Paper 13-307, AAS/AIAA Spaceflight Mechanics Meeting, Kauai, Hawaii, 10 - 14 February 2013.
11. Schoenenberger, M., "Preliminary Trajectory Reconstruction Results of the Mars Science Laboratory Entry Vehicle," AAS Paper 13-306, AAS/AIAA Spaceflight Mechanics Meeting, Kauai, Hawaii, 10 - 14 February 2013.